

**Insight into PM_{2.5} Sources by Applying Positive
Matrix Factorization (PMF) at an Urban and
Rural Site of Beijing**

**Deepchandra Srivastava¹, Jingsha Xu¹, Tuan V. Vu^{1,2}
Di Liu^{1,3}, Linjie Li³, Pingqing Fu⁴, Siqi Hou¹, Zongbo Shi^{1,*}
and Roy M. Harrison^{1†*}**

**¹ School of Geography Earth and Environmental Science, University
of Birmingham, Birmingham, B15 2TT
United Kingdom**

**² Now at: School of Public Health, Imperial College London, London
United Kingdom**

**³ Institute of Atmospheric Physics, Chinese Academy of Sciences
Beijing, 100029, China**

**⁴ Institute of Surface-Earth System Science, Tianjin University,
Tianjin 300072, China**

**† Also at: Department of Environmental Sciences / Centre of Excellence in Environmental
Studies, King Abdulaziz University, PO Box 80203, Jeddah, 21589, Saudi Arabia**

**Corresponding author: E-mail: r.m.harrison@bham.ac.uk (Roy M. Harrison) and
z.shi@bham.ac.uk (Zongbo Shi)**

31 ABSTRACT

32 This study presents the source apportionment of PM_{2.5} performed by PMF on data collected at an
33 urban (Institute of Atmospheric Physics - IAP) and a rural site (Pinggu-PG) in Beijing as part of the
34 Atmospheric Pollution and Human Health in a Chinese megacity (APHH-Beijing) field campaigns.
35 The campaigns were carried out from 9th November to 11th December 2016 and 22nd May to 24th June
36 2017. The PMF included both organic and inorganic species, and a seven-factor output provided the
37 most reasonable solution for the PM_{2.5} source apportionment. These factors are interpreted to be
38 traffic emissions, biomass burning, road dust, soil dust, coal combustion, oil combustion and
39 secondary inorganics. Major contributors to PM_{2.5} mass were secondary inorganics (IAP: 22%; PG: -
40 24%), biomass burning (IAP: 36%~~30~~; PG: 30%~~36~~), and coal combustion (IAP: 20%; -PG: 21%)
41 sources during the winter period at both sites. Secondary inorganics (48%), road dust (20%) and coal
42 combustion (17%) showed the highest contribution during summer at PG, while PM_{2.5} particles were
43 mainly composed of soil dust (35%) and secondary inorganics (40%) at IAP. Despite this, factors that
44 were resolved based on metal signatures were not fully resolved and indicate a mixing of two or more
45 sources. PMF results were also compared with sources resolved from another receptor model (i.e.
46 CMB) and PMF performed on other measurements (i.e. online and offline aerosol mass spectrometry
47 (AMS)) and showed a good agreement for some but not all sources. The biomass burning factor in
48 PMF may contain aged aerosols as a good correlation was observed between biomass burning and
49 oxygenated fractions ($r^2=0.6-0.7$) from AMS. The PMF failed to resolve some sources identified by
50 the CMB and AMS, and appears to overestimate the dust sources. A comparison with earlier PMF
51 source apportionment studies from the Beijing area highlights the very divergent findings from
52 application of this method.

53 **Key words:** Source apportionment; PM_{2.5}; Beijing; PMF; CMB; online AMS; offline AMS

54

1. INTRODUCTION

Atmospheric particulate matter (PM) is composed of various chemical components and can affect air quality (and consequently human health), visibility, and ecosystems (Boucher et al., 2013; Heal et al., 2012). Through absorption and scattering of solar radiation and by affecting clouds, PM also have a major impact on the climate, and thus the hydrological cycle. PM with an aerodynamic diameter less than $2.5\text{ }\mu\text{m}$ ($\text{PM}_{2.5}$) is given special attention due to its adverse effects on human health as it can penetrate deep into human lungs when inhaled. Several recent studies have indicated that many adverse health outcomes, such as respiratory and cardiovascular morbidity and mortality, are related to long-term exposure to PM (Lu et al., 2021; Wang et al., 2016; Xing et al., 2016; Xie et al., 2019). In addition, over a million premature deaths per year are reported in China due to poor air quality (GBD MAPS Working Group, 2016). Beijing, the capital city of China, is a megacity with approximately 21 million inhabitants that are regularly exposed to severe haze events. For example, pollution episodes (defined as two or more consecutive days where the average $\text{PM}_{2.5}$ concentration exceeds $75\text{ }\mu\text{g m}^{-3}$) were observed between April 2013 to March 2015 (Batterman et al., 2016). $\text{PM}_{2.5}$ concentrations have reached $1,000\text{ }\mu\text{g m}^{-3}$ in some heavily polluted areas of Beijing (Ji et al., 2014). In addition, a study compared the number of cases of acute cardiovascular, cerebrovascular, and respiratory diseases in the Beijing Emergency Center and haze data from Beijing Observatory between 2006 and 2013. Their results showed a rising trend, highlighting the average number of cases per day for all three diseases was higher on hazy days than on non-hazy days (Zhang et al., 2015a). Therefore, major control measures were implemented to reduce $\text{PM}_{2.5}$ pollution in Beijing (Vu et al., 2019). Recently, one-third of Chinese cities in 2020 were kept under lockdown to prevent the transmission of COVID-19 virus, which strictly curtailed personal mobility and economic activities. The lockdown led to an improvement in air quality and managed to bring down the levels of $\text{PM}_{2.5}$. Despite these improvements, $\text{PM}_{2.5}$ concentrations during the lockdown periods remained higher than the World Health Organization recommendations, suggesting much further effort is

80 needed (He et al., 2020; Le et al., 2020; Shi et al., 2021). A quantitative source apportionment
81 provides key information to support such efforts.

82

83 Receptor models are widely used for source apportionment of PM_{2.5}. These methods include positive
84 matrix factorization (PMF) (Paatero, 1997; Paatero and Tapper, 1994), principal component analysis
85 (PCA) (Lee et al., 2011), chemical mass balance (CMB) (Watson et al., 1990), and UNMIX (Herrera
86 Murillo et al., 2012). Among these methods, PMF is a widely used multivariate method that can
87 resolve the dominant positive factors without prior knowledge of sources. Previous PMF studies,
88 based on high resolution Aerosol Mass Spectrometer data, have provided valuable information on the
89 sources of PM in urban Beijing and its surrounding areas (Zhang et al., 2015b; Huang et al., 2010b;
90 Sun et al., 2010; Sun et al., 2013; Zhang et al., 2013; Zhang et al., 2014; Zhang et al., 2017; Zhang et
91 al., 2016; Hu et al., 2016; Qiu et al., 2019). However, the factors that influence haze formation and
92 related sources remain unclear due to its inherent complexity (Tie et al., 2017; Sun et al., 2014). Filter-
93 based PMF studies provide a valuable tool for identifying sources of airborne particles, by utilising
94 size-resolved chemical information (Li et al., 2019; Ma et al., 2017a; Tian et al., 2016; Yu et al.,
95 2013; Song et al., 2007; Song et al., 2006). These source apportionment studies have predominantly
96 used OC (organic carbon), EC (elemental carbon), water soluble ions and metals as the input data
97 matrix to explore the co-variances between species and their associated sources, but to the best of our
98 knowledge, the use of organic markers in PMF has not been explored extensively in Beijing. The use
99 of organic molecular markers in PMF has enhanced our understanding of the PM fraction as they can
100 be source specific (Shrivastava et al., 2007; Jaekels et al., 2007; Zhang et al., 2009; Wang et al.,
101 2012; Srimuruganandam and Shiva Nagendra, 2012; Schembari et al., 2014; Laing et al., 2015;
102 Waked et al., 2014; Srivastava et al., 2018) and could potentially offer a clearer link between factors
103 and sources.

104

105 This study presents the results obtained from the PMF model applied to a filter-based dataset collected
106 in the Beijing metropolitan area at two sites, urban and rural. The study provides source
107 apportionment results from both urban and rural locations in Beijing including their temporal and
108 spatial variations. In addition, the study also presents a short summary of previously published filter-
109 based studies conducted in the Beijing metropolitan area and their major outcomes. A comparison of
110 the present PMF results was also made with other source apportionment approaches or applications
111 of PMF to other datasets, with an aim to discuss the existing PM sources in the Beijing metropolitan
112 area, including focusing on the strengths and weaknesses of the source apportionment approach
113 employed.

114

115 **2. METHODOLOGY**

116 Details about the sampling site, measurements, sample collection and analytical procedures are
117 reported elsewhere (Shi et al., 2019; Xu et al., ~~2020~~2021; Wu et al., 2020), and hence only the
118 essential information is presented in this section.

119

120 **2.1 Sampling Site and Sample Collection**

121 The PM_{2.5} sampling was conducted simultaneously at the urban and rural sites from 9th November to
122 12th December 2016 and 22nd May to 24th June 2017 as part of the Atmospheric Pollution and Human
123 Health in a Chinese megacity (APHH-Beijing) field campaigns (Shi et al., 2019) (Figure S1). The
124 urban sampling site (116.39E, 39.98N) - the Institute of Atmospheric Physics (IAP) of the Chinese
125 Academy of Sciences in Beijing, represents typical condition of central Beijing, there are various
126 roads nearby including a highway road approximately 200 m away. The rural Pinggu site (PG)
127 (40.17N, 117.05E) is located in Xibaidian village. This site is approximately 60 km to the north-east
128 of Beijing city centre and about 4 km north-west of the Pinggu town centre. The site is surrounded

129 by trees and farmland. In addition, residents mainly use coal and biomass for heating and cooking in
130 individual homes.

131
132 24-hour PM_{2.5} samples were collected every day on pre-baked quartz filters (Pallflex, 8×10 inch) and
133 47 mm PTFE filters (flow rate of 15.0 L min⁻¹) using high volume (Tisch, USA, flow rate of 1.1 m³
134 min⁻¹) and medium volume (Thermo Scientific Partisol 2025i) air sampler. Field blanks were also
135 collected during the sampling campaign at both sites. The quartz filters were then analyzed for organic
136 tracers, OC/EC and ion species. PTFE filters were used for the determination of PM_{2.5} mass and
137 metals. Details on preparation and conservation of these filter samples have already been reported
138 elsewhere (Wu et al., 2020; Xu et al., ~~2020~~2021).

139
140 Real time composition of non-refractory PM₁ particles (NR-PM₁) was measured using an Aerodyne
141 aerosol mass spectrometer (AMS) at a time resolution of 2.5 min. The operational details on the AMS
142 measurements have been given elsewhere (Xu et al., 2019). In addition, the measurements of gaseous
143 species such as O₃, CO, NO, NO₂ and SO₂ were performed using gas analyzers. The meteorological
144 parameters including temperature (T), relative humidity (RH), wind speed (WS), and wind direction
145 (WD) were also measured at both sites.

146

147 **2.2 Analytical Procedure**

148 In all 62 and 72 chemical species were quantified in each PM_{2.5} sample from IAP and PG,
149 respectively. This included EC/ OC, 36 organic tracers, 7 major inorganic ions (Na⁺, K⁺, Ca²⁺, NH₄⁺,
150 Cl⁻, NO₃⁻ and SO₄²⁻) and 17 metallic elements (V, Cr, Co, Mn, Ni, Cu, Zn, As, Br, Sr, Ag, Cd, Sn,
151 Sb, Ba, Hg and Pb) at IAP. Similarly, the identified species at PG included EC/OC, 51 organic tracers,
152 7 major inorganic ions and 12 metallic elements (V, Cr, Co, Mn, Ni, Cu, Zn, As, Sr, Sb, Ba, and Pb).
153 EC and OC measurements were performed using a Sunset lab analyser (model RT-4) and DRI multi-

154 wavelength thermal-optical carbon (model 2015) analyser based on the EUSAAR2 (European
155 Supersites for Atmospheric Aerosol Research) transmittance protocol at both sites, IAP and PG,
156 respectively, following the procedure explained by Paraskevopoulou et al. (2014). Major inorganic
157 ions and metallic elements were analysed using an ion chromatograph (Dionex, Sunnyvale, CA,
158 USA) and Inductively coupled plasma-mass spectrometer (ICP-MS) at both sites, respectively. Major
159 crustal elements including Al, Si, Ca, Ti and Fe were determined by X-ray fluorescence spectrometer
160 (XRF).

161
162 Organic tracers at IAP included n-alkanes 11 C₂₄-C₃₄, 2 hopanes, 17 PAHs, 3 anhydrous sugars
163 (levoglucosan, mannosan, galactosan), 2 fatty acids (palmitic acid, stearic acid) and cholesterol.
164 These organic tracers were analysed by gas chromatography mass spectrometry (GC/MS, Agilent
165 7890A GC plus 5975C mass-selective detector) coupled with a DB-5MS column (30 m × 0.25 mm ×
166 0.25 µm) following the protocol explained in Xu et al. (2020). At PG, organic tracers were analysed
167 based on the method reported by Wu et al. (2020) using GC/MS (Agilent GC-6890N plus MSD-
168 5973N) coupled with a HP-5MS column (30 m × 0.25 mm × 0.25 µm). This included quantification
169 of similar species (12 n-alkanes C₂₄-C₃₅, 9 hopanes, 22 PAHs, 3 anhydrous sugars (levoglucosan,
170 mannosan, galactosan), 4 fatty acids (palmitic acid, stearic acid, linoleic acid, oleic acid) and
171 cholesterol) with few additional ones. Recoveries for the identified organic tracers ranged from 70-
172 100% and 80-110 %, at IAP and PG, respectively. Field blank were also analysed as part of quality
173 control and demonstrated very low contamination (<5%).

174
175 In addition, one or two punches of PM_{2.5} filter sample were also analysed offline using AMS to
176 investigate the water-soluble OA (WSOA) mass spectra following the procedure explained
177 previously (Qiu et al., 2019).

178

179 2.4 Positive Matrix Factorization

180 Detailed information on the receptor modelling methods used within this study can be found
 181 elsewhere (Paatero and Tapper, 1994; Hopke, 2016). Positive matrix factorization (PMF) is a
 182 multivariate factor analysis tool and based on a weighted least square fit, where the weights are
 183 derived from the analytical uncertainty. The best model solution was obtained by minimizing
 184 residuals obtained between modeled and observed input species concentrations Estimation of
 185 analytical uncertainties for the filter-based measurements was calculated using Eq. (1) (Polissar et al.,
 186 1998).

$$187 \quad \sigma_{ij} = \begin{cases} \frac{5}{6}LD_j & \text{if } X_{ij} < LD_j \\ \sqrt{(0.5 * LD_j)^2 + (EF_j X_{ij})^2} & \text{if } X_{ij} \geq LD_j \end{cases} \quad \text{Eq. (1)} \quad 188$$

189 where LD_j is the detection limit for compound j and EF_j is the error fraction for the compound j . The
 190 detection limits of all compounds used in the PMF model is given in Table S1 (SI). The U.S.
 191 Environmental Protection Agency (US-EPA) PMF 5.0 software was used in this work to perform the
 192 source apportionment.
 193

194 ***Selection of the input data.*** The selection of species used as input data for the PMF analysis is
 195 important and can significantly influence the model results (Lim et al., 2010). The following set of
 196 criteria were used for the selection of the input species: signal to noise ratio (S/N) (Paatero and Hopke,
 197 2003), major PM chemical species, compounds with maximum data points above the detection limit
 198 and those being considered as specific markers of a given source (e.g., levoglucosan, picene) (Oros
 199 and Simoneit, 2000; Simoneit, 1999) were selected. These steps were taken to limit the input data
 200 matrix according to the total number of samples (n=133); some species were also not included if they
 201 belonged to a single source and correlated with another marker of this source. A total of 31 species
 202 were used in the model ($PM_{2.5}$, OC, EC, K^+ , Na^+ , Ca^{2+} , NH_4^+ , NO_3^- , SO_4^{2-} , Cl^- , Ti, V, Mn, Ni, Zn, Pb,
 203

204 Cu, Fe, Al, C26, C29, C31, 17 α (H)-22,29,30-trisnorhopane, 17 β (H), 21 α (H)-30-norhopane, chrysene,
205 benzo(b)fluoranthene, benzo(a)pyrene, picene, corene, levoglucosan, and stearic acid). The
206 concentration of PM_{2.5} was included as a total variable in the model (with large uncertainties) to
207 directly determine the source contributions to the daily mass concentrations.

208
209 ***Selection of the final solution.*** As normally recommended, a detailed evaluation of factor profiles,
210 temporal trends, fractional contribution of major species to each factor and correlations with external
211 tracers, were investigated carefully to select the appropriate number of factors.

212
213 A few constraints were also applied to the base run to obtain clearer chemical source profiles in the
214 final solution. The general framework for applying constraints to PMF solutions has already been
215 discussed elsewhere (Amato et al., 2009; Amato and Hopke, 2012). The changes in the Q values were
216 considered here as a diagnostic parameter to provide insight into the rotation of factors. All model
217 runs were carefully monitored by examining the Q values obtained in the robust mode. To limit
218 change in the Q -value, only “soft pulling” constraints were applied. The change in the Q -robust was
219 < 1%, which is acceptable as per PMF guidelines (< 5%) (Norris et al., 2014). Finally, three criteria
220 were used to select the optimal solution, including correlation coefficient (r) between the measured
221 and modelled species, bootstrap and t-test (two-tailed paired t-test) performed on the base and
222 constraint runs, as explained previously (Srivastava et al., 2018).

223

224 **2.5 Back trajectories and Geographical Origins**

225 The geographical origin of selected identified sources and pollutants was investigated using
226 concentration-weighted trajectory (CWT), non-parametric wind regression (NWR), and cluster
227 analysis methods. NWR combines ambient concentrations with co-located measurements of wind
228 direction and speed and highlights wind sectors that are associated with high measured concentrations
229 (Henry et al., 2009). The general principle is to smooth the data over a fine grid, so that a weighted

concentration could be estimated by any wind direction (ϕ)/wind speed (v) couple, where the weighing coefficients are determined through Gaussian-like functions. CWT and cluster analysis assess the potential transport of pollution over large geographical scale (Polissar et al., 2001). These approaches combine atmospheric concentrations measured at the receptor site with back trajectories and residence time information and help to geographically evaluate air parcels responsible for high concentrations. For this purpose, hourly 24-h back trajectories arriving at 200 m above sea level were calculated from the PC-based version of HYSPLIT v4.1 (Stein et al., 2015; Draxler, 1999). NWR, CWT calculations and cluster analysis, were performed using the ZeFir Igor package (Petit et al., 2017).

239

240 **2.6 Other Receptor Modelling Approaches**

Sources were also resolved at both sites separately using another receptor model known as chemical mass balance (CMB) as well as PMF performed on high resolution AMS data collected at IAP. Details on sources resolved using these approaches are reported elsewhere (Wu et al., 2020; Xu et al., 2020; Sun et al., 2020).

245

Briefly, CMB is based on a linear least squares approach and accounts for uncertainties in both, source profiles and ambient measurements to apportion the sources of OC. The US EPA CMB8.2 software was used for this purpose at both sites. The source profiles applied in the model were taken from local studies to better represent the sources, including profiles of straw burning (Zhang et al., 2007), wood burning (Wang et al. 2009), gasoline and diesel vehicles (Cai et al. 2017), industrial and residential coal combustion (Zhang et al., 2008), and cooking (Zhao et al., 2015). Only the source profile for vegetative detritus (Rogge et al. 1993; Wang et al., 2009) was not available from local studies. The selected fitting species included EC, anhydrous sugar (levoglucosan), fatty acids, PAHs, hopanes and alkanes

255 3. RESULTS AND DISCUSSION

256 3.1 Overview on PM Sources in Beijing based on the Current Source Apportionment Study

257 A seven-factor output provided the most reasonable solution for the PM_{2.5} source apportionment
258 performed on the combined dataset from IAP and PG (Figures 1 and 2).

259

260 Based on the factor profiles, we identified traffic emissions, biomass burning, road dust, soil dust,
261 coal combustion, oil combustion and secondary inorganics. For the same dataset, solutions with six
262 sources were less explanatory and some factors were mixed. Conversely, an increase in the number
263 of factors led to the split of meaningful factor profiles. In the final solution, the comparison of the
264 reconstructed PM_{2.5} contributions from all sources with measured PM_{2.5} concentrations for different
265 seasons at both sites showed good mass closure ($r^2 = 0.61-0.91$, slope = 0.99-1.12, $p < 0.05$, ODR
266 (orthogonal distance regression)). A low r^2 (0.61) value was observed for the summer period at IAP
267 (Figure S2). This may be due to the inability of PMF to model low concentrations observed for
268 sources such as biomass burning and coal combustion during the summer. In addition, most of the
269 species showed good agreement with measured concentrations (Table S2). Bootstrapping on the final
270 solution showed stable results with more than 95 out of 100 bootstrap mapped factors (Table S3).
271 Finally, no significant difference ($p > 0.05$) was observed in the factor chemical profiles between the
272 base and the constrained runs (Table S4).

273

274 Overall, secondary inorganics, biomass burning, and coal combustion sources were the main
275 contributors to the total PM_{2.5} mass during winter (Figure 3). These sources accounted for 22%, 36%,
276 20%, and 24%, 30%, 21% of PM_{2.5} mass at IAP and PG, respectively. Secondary inorganics, road
277 dust and coal combustion showed the highest contribution during summer at PG, while PM_{2.5} particles
278 were mainly composed of soil dust and secondary inorganics at IAP. Identified aerosol sources, factor
279 profiles and temporal evolutions are discussed below. Note, PMF was carried out on the combined
280 datasets and thus only provides a single set of factor profiles for both sites. Similar to previous studies

281 (Li et al., 2019; Ma et al., 2017a; Tian et al., 2016; Yu et al., 2013; Liu et al., 2019; Zhang et al.,
282 2013), neither secondary organic aerosol nor cooking emissions were identified, and given the good
283 mass closure must be present within other source categories.

284
285 **Coal combustion.** Coal combustion was identified based on it accounting for a high proportion of
286 PAHs (27-78%), especially picene (78%) as a specific marker of coal combustion (Oros and
287 Simoneit, 2000), together with significant amount of OC (45%) and EC (29%) (Figure 1). This factor
288 also made a substantial contribution to n-alkanes (28-58%), stearic acid (64%) and hopanes (53-56%),
289 as these compounds are also abundant in coal smoke (Bi et al., 2008; Zhang et al., 2008; Oros and
290 Simoneit, 2000; Guo et al., 2015).

291
292 The coal combustion factor accounted for 20% of the PM mass ($16.0 \mu\text{g m}^{-3}$) at the urban site IAP
293 during winter and followed typical seasonal variations. However, the contributions of this source to
294 $\text{PM}_{2.5}$ mass were broadly similar (21% vs 17%, Figure 3) at PG during both seasons, while the average
295 concentrations were higher in winter than summer ($19.4 \mu\text{g m}^{-3} > 4.6 \mu\text{g m}^{-3}$). Due to a lack of
296 infrastructure at the rural site PG, the residents still use coal for cooking and heating purposes at the
297 time of sampling (Shi et al., 2019). There is a reduction in coal usage for heating due to elevated
298 temperatures in the summertime, leading to low levels of this factor. But the similar contribution at
299 the rural site could be linked to consistent cooking activities throughout the year (Figure 2) (Shi et
300 al., 2019; Tao et al., 2018). These results were in good agreement with previous observations reported
301 at the same urban site (18%) (Ma et al., 2017a; Tian et al., 2016). In addition, similar contributions
302 were also observed at other urban locations around Beijing (Wang et al., 2008; Liu et al., 2019).

303
304 This factor also included significant contributions from levoglucosan (60%). Levoglucosan, a major
305 pyrolysis product of cellulose, and has been proposed as molecular marker of biomass burning
306 aerosols (Simoneit, 1999). A study conducted in China suggested that residential coal combustion
307 can also contribute significantly to levoglucosan emissions, based on both source testing and ambient

308 measurements (Yan et al., 2018). Therefore, it is expected that the contribution of levoglucosan is
309 probably linked to residential coal use for cooking in this case. It is also possible that the high
310 contribution of levoglucosan could also be linked to model bias as the PMF model only provides an
311 average factor profiles for both sites irrespective of their nature (rural vs. urban) and different
312 sampling periods (summer vs. winter).

313
314 This was further supported as NWR and CWT analysis showed similar results, mostly dominated by
315 a northerly flow during the winter period at both sites. High concentrations of this source and
316 levoglucosan were observed at low wind speeds (Figure S3), indicating the significant role of local
317 activities. Higher levels were observed at the rural site PG ($19.4 \mu\text{g m}^{-3}$ vs $16.0 \mu\text{g m}^{-3}$ at the urban
318 site). However, a south-westerly flow was dominant during summer and could be related to transport
319 of air masses from the Hebei province where a large number of industries operate.

320
321 **Oil combustion.** The oil combustion factor profile included high contributions to V (79%) and Ni
322 (70%) (see Figure 1). V and Ni are widely used markers for oil combustion in residential, commercial
323 and industrial applications (Viana et al., 2008; Mazzei et al., 2008; Pant et al., 2015; Huang et al.,
324 2021). The V/Ni ratio obtained in this study was 0.9, close to the previously obtained ratio for residual
325 oil used in power plants (Swietlicki and Krejci, 1996). Results suggest this source might be attributed
326 to residual oil combustion linked to industrial activities as a large number of highly polluting
327 industries are still located in the Beijing neighbourhood (Li et al., 2019). CWT and NWR analysis
328 suggested the influence of regional transport at both sites, highlighting the dominance of south
329 westerly and south easterly flows during the winter and summer at both sites (Figure S4).

330
331 The source did not show any seasonal pattern (Figure 2), and accounted for 2% ($1.4 \mu\text{g m}^{-3}$) and 6%
332 ($1.6 \mu\text{g m}^{-3}$) at IAP, and 8% ($7.1 \mu\text{g m}^{-3}$) and 9% ($2.1 \mu\text{g m}^{-3}$) at PG of the $\text{PM}_{2.5}$ mass during winter
333 and summer, respectively (Figure 3). The contribution of this source to the PM mass was within the

334 similar range to the previous study conducted at the same urban site (contribution 4.7%) (Li et al.,
335 2019), which also found a high proportion of V attributed to the identified source.

336
337 **Biomass burning.** The biomass burning factor was characterized by high contributions to Cl^- (74%),
338 K^+ (27%) and levoglucosan (25%) (Figure 1). This factor also made significant contributions to PAHs
339 (Chry (66%), B[b]F (66%), Cor (68%)) and followed a clear seasonal variation with a higher
340 contribution in winter (Figure 2). It accounted for 36 % ($29.0 \mu\text{g m}^{-3}$) and 30% ($27.3 \mu\text{g m}^{-3}$) of the
341 $\text{PM}_{2.5}$ mass during the wintertime at IAP and PG, respectively (Figure 3), while the contribution
342 during the summertime was extremely low. This was expected due to elevated temperature during
343 the summer period and reduction in biomass burning activities. In addition, NO_3^- (24%), and NH_4^+
344 (24%) also contributed significantly to the biomass burning factor. Biomass burning is an important
345 natural source of NH_3 (Zhou et al., 2020) which rapidly reacts with HNO_3 to form NH_4NO_3 aerosols.
346 The presence of NH_4NO_3 aerosols in biomass burning plumes, has also been reported previously
347 (Paulot et al., 2017; Zhao et al., 2020).

348
349 It was unexpected to observe a low contribution of levoglucosan, a known biomass burning marker,
350 to this factor. However, model bias and the contribution of other relevant sources to levoglucosan
351 could cause such observations, as discussed above. K^+ is also produced from the combustion of wood
352 lignin and has been used extensively as an inorganic tracer to apportion biomass burning contributions
353 to ambient aerosol (Zhang et al., 2010; Lee et al., ~~2008b~~2008a). However, the contribution of K^+ to
354 this factor was ~~not~~ relatively low, possibly because K^+ has also other sources, such as soil dust (Duvall
355 et al., 2008). Cl^- can be emitted from both coal combustion and biomass burning, especially during
356 the cold period in Beijing (Sun et al., 2006). It is also important to note that high Cl^- levels observed
357 in this factor could be associated with coal combustion as Cl^- has been used to represent coal
358 combustion activities in China (Wang et al., 2008). If we consider this, high Cl^- levels related to the
359 coal combustion factor should have also shown a significant contribution to PM mass during the

360 summertime at the rural site (PG) as residents near the rural site mostly use coal and biomass for
361 cooking activities as discussed above, but they do not. Results suggest this factor can be attributed
362 mainly to biomass burning aerosols in the Beijing metropolitan area, but some influence of coal
363 combustion signals cannot be ignored. Back trajectory analysis also confirmed the local origin of this
364 source during the wintertime at both sites (Figure S5).

365

366 The source contribution reported in the present study was higher than that found in earlier studies in
367 Beijing (11-20%) (Li et al., 2019; Ma et al., 2017a; Tian et al., 2016; Yu et al., 2013; Song et al.,
368 2007; Song et al., 2006; Liu et al., 2019), suggesting some inclusion of coal burning. As both these
369 sources follow a similar typical seasonal variation, i.e., high concentration during the cold period, it
370 makes their separation difficult due to correlation.

371

372 ***Secondary inorganics.*** Secondary inorganics were typically characterized by high contributions to
373 NO_3^- , SO_4^{2-} and NH_4^+ (55%, 56% and 56% of the total species mass, respectively) (Figure 1). This
374 factor showed a temporal variation, with remarkably high concentrations observed during the period
375 of high relative humidity (RH) and low ozone concentration in the winter (Figure S6). The
376 heterogeneous reactions on pre-existing particles in the polluted environment under high RH and low
377 ozone conditions have been shown to play a key role in the formation of secondary aerosols compared
378 to gas-phase photochemical processes (Sun et al., 2013; Niu et al., 2016; Ma et al., 2017b). Therefore,
379 aqueous phase processes may be the major formation pathway for secondary inorganic aerosols in
380 Beijing during the study period. Additionally, the factor showed a similar contribution (22-24%) to
381 PM mass in winter at both sites. This value is lower than the value reported by Liu et al. (2019) at the
382 other urban location (44%) in Beijing as a part of same APHH-Beijing campaign, although it should
383 be noted that the sampling site and dates of sampling differed. We also noticed the source profile
384 reported by Liu et al. (2019) contained a majority of all measured secondary inorganic species (>70%)
385 as well as 20% of OC while the factor identified in the present study only accounted for ~55% of

secondary inorganic species and 11% of OC with remaining fractions identified in other factors. Thus, although the identification of the factor was “secondary” in both studies, they do not represent exactly the same source. The modelled difference in the contribution of this factor to PM mass may also be related to the uncertainties of the input species: a filter-based dataset was used in the present study while Liu et al., (2019) used online measurements. Additionally, the factor showed a similar contribution (22–24%) to PM mass in winter at both sites. This value is lower than the value reported by Liu et al. (2019) at the other urban location (44%) in Beijing as a part of same APHH Beijing campaign (Liu et al., 2019), although it should be noted that the sampling site and dates of sampling differed.

The highest contribution to the PM mass was observed during the summertime, with an average concentration of $11.1 \mu\text{g m}^{-3}$ (40%) and $13.2 \mu\text{g m}^{-3}$ (48%) at IAP and PG, respectively (Figure 3).

Traffic emissions. The traffic emissions factor showed relatively high contributions to metallic elements, such as Zn (47%), Pb (57%), Mn (27%) and Fe (22%) (Figure 1). Zn is a major additive to lubricant oil. Zn and Fe can also originate from tyre abrasion, brake linings, lubricants and corrosion of vehicular parts and tailpipe emission (Pant and Harrison, 2012; Pant and Harrison, 2013; Grigoratos and Martini, 2015; Piscitello et al., 2021). As the use of Pb additives in gasoline has been banned since 1997 in Beijing, the observed Pb emissions may be associated with wear (tyre/brake) rather than fuel combustion (Smichowski et al., 2007). These results suggest the contribution of both exhaust and non-exhaust traffic emissions to this factor. Further insight on the type of non-exhaust emissions is hard to predict as these metal concentrations vary according to several parameters, such as traffic volume and patterns, vehicle fleet characteristics and the climate and geology of the region (Duong and Lee, 2011).

412 Traffic sources accounted for 9% and 6% of $\text{PM}_{2.5}$ mass during the winter and summertime at IAP
413 (Figure 3), corresponding to an average concentration of $7.4 \mu\text{g m}^{-3}$ and $1.8 \mu\text{g m}^{-3}$, respectively. In
414 addition, a low contribution (4%) was observed at PG during both seasons as PG experiences a low
415 traffic volume. The contribution of the traffic source to the $\text{PM}_{2.5}$ mass was found to be low compared
416 to other studies conducted in the Beijing area; (14-20%) (Li et al., 2019; Tian et al., 2016; Yu et al.,
417 2013; Liu et al., 2019), with the exception of a study by Ma et al. (2017a) where a similar contribution
418 was reported. The observed low contribution was further supported as a recent study also confirms
419 that road traffic remains a dominant source of NO_x and primary coarse PM, however, it only accounts
420 a relatively small fraction of $\text{PM}_{2.5}$ mass at urban locations in Beijing (Harrison et al., 2021). It should
421 be noted that nitrate that can be formed from NO_x emitted from road traffic is not included in this
422 factor. Despite the low factor contribution, the resolved chemical profile of this source was consistent
423 with previously identified profiles linked to road traffic emissions in the Beijing area (Ma et al.,
424 2017a; Yu et al., 2013). We noticed that OC/EC contribution in this factor is relatively low, while it
425 may be higher in traffic emissions. However, given the modern gasoline fleet in Beijing (Jing et al.,
426 2016), it is not unexpected to observe low OC and EC contribution. We do expect higher OC and EC
427 contribution from diesel vehicles. In addition, there was no obvious seasonal variation as expected,
428 though slightly higher concentrations were observed in the cold period, probably due to the typical
429 atmospheric dynamics, and consequent poorer dispersion at this time of year.

430
431 Metallic elements such as Mn, Fe and Zn were also used previously to indicate industrial activities
432 (Li et al., 2017; Yu et al., 2013). Back trajectory analysis reveals the influence of local emissions with
433 a slight regional transport during the winter period at both sites, dominated by north easterly flow
434 (Figure S7). Therefore, there is a possibility that these elements could also come from the Hebei
435 province where a large number of smelter industries are located. North-easterly and south-easterly
436 flows were dominant during the summer period at IAP and PG with possible regional influence. These

437 observations suggest that indeed this factor contains traffic aerosols, though a significant influence
438 of industrial emissions cannot be ruled out.

439
440 **Road dust.** This factor makes a major contribution to crustal species, such as Na⁺, Al and Fe (60%,
441 48% and 34% of species in this factor respectively) suggesting this factor may represent the
442 characteristics of a dust related source as reported previously (Kim and Koh, 2020). Such a high
443 contribution of Na⁺ in the identified factor was unexpected. Na is a major element of sea salt, sea-
444 spray and marine aerosols (Viana et al., 2008), and has also been found to be enriched in fine
445 particulates from coal combustion (Takuwa et al., 2006). It is notable that a high proportion of Na⁺
446 was attributed to road dust in a previous study conducted at the same urban site (Tian et al., 2016),
447 and a crustal source seems likely, but has not been confirmed. In addition, the given factor also
448 included significant contributions to Mn, Pb and Zn (26%, 23% and 20% of species in this factor
449 respectively), which are associated with brake and tyre wear as mentioned above (Pant and Harrison,
450 2012; Pant and Harrison, 2013; Grigoratos and Martini, 2015; Piscitello et al., 2021). High
451 concentrations of Zn and Pb have also been reported for particles emitted from asphalt pavement
452 (Canepari et al., 2008; Sörme et al., 2001). In addition, the ratio of Fe/Al observed in the factor
453 chemical profile was 1.26, much higher than the value observed in the earth's crust (0.6), suggesting
454 an anthropogenic origin of some Fe (Sun et al., 2005). This is likely as processes associated with
455 vehicles, such as tyre/brake wear and road abrasion, can contaminate soil with metals, as the urban
456 sampling site is located close to roads suggesting the resolved factor is likely linked to road dust
457 emissions. These metals (Fe and Al) can also have industrial sources as already reported in the Beijing
458 area (Wang et al., 2008; Tian et al., 2016; Yu et al., 2013; Li et al 2019). The Beijing-Tianjin-Hebei
459 region is the largest urbanised megalopolis region in northern China, and home to many iron and steel
460 making industries. Fe is characteristic components of iron and steel industry emissions (Li et al.,
461 2019) while Al may also come from metal processing (Yu et al., 2013). However, disentangling the
462 influence of industrial emissions would require further investigation.

463
464 This source also made significant contributions to OC, EC and SO_4^{2-} (11-19%) (Figure 1) and was
465 consistent with the road dust source profiles observed previously in the Beijing area (Song et al.,
466 2006; Song et al., 2007; Tian et al., 2016; Yu et al., 2013). This factor accounted for 20% of the $\text{PM}_{2.5}$
467 mass during the summertime ($5.5 \mu\text{g m}^{-3}$) with exceptionally low contribution (3%) during the cold
468 period at PG (Figure 3). However, the factor contribution at IAP was similar during both seasons. In
469 addition, the contribution to PM mass at IAP in this study was similar to that reported by Tian et al.
470 (2016) and the studied urban site in both cases was the same. Crustal dust mass was also estimated
471 based on the concentrations of Al, Si, Fe, Ca, and Ti using the equation below (Chan et al., 1997).

472
$$\text{Crustal dust} = 1.16(1.9\text{Al} + 2.15\text{Si} + 1.41\text{Ca} + 1.67\text{Ti} + 2.09\text{Fe})$$

473
474 [A g](#)Good correlation was observed between the estimated crustal dust and this factor during both
475 seasons at PG (rural, winter: $r^2 = 0.78$, m (slope) =0.9; summer: $r^2 = 0.94$, m=0.5) and IAP (urban,
476 winter: $r^2 = 0.51$, m=1.3; summer: $r^2 = 0.68$, m=1.2), highlighting that this may also contain a
477 significant fraction of crustal dust (Figure S8). This suggests [that](#) the identified factor is not resolved
478 cleanly and contains a mixed characteristic of road dust and crustal dust.

479
480 **Soil dust.** This factor mainly represents wind-blown soils and was typically characterized by a high
481 contribution to crustal elements, such as Ti (63%), Ca^{2+} (41%), Fe (27%) and Al (17%) (Figure 1).
482 In addition, the contributions to Mn and Zn in the factor profile (Mn=24%, Zn=15%) suggest that the
483 given source also included resuspended road dust but probably to a lesser extent. ~~No clear seasonal~~
484 ~~variation was observed.~~ This source also showed a significant contribution to n-alkanes (e.g., C29,
485 C31), derived from epicuticular waxes of higher plant biomass (Kolattukudy, 1976; Eglinton et al.,
486 1962), with the highest contribution (37%) to C31. This suggests the presence of plant derived organic
487 matter in the soil dust, which is also consistent with a high contribution to OC (15%).

488

489 No clear seasonal variation was observed at PG. However, this factor showed a high contribution
490 (35%, $9.8 \mu\text{g m}^{-3}$) to $\text{PM}_{2.5}$ mass during the summertime at IAP, while the contribution during other
491 seasons at both sites was less than 10% (Figure 3). The factor profile resolved here was similar to the
492 profile reported by Ma et al. (2017a) for soil dust, but their soil dust factor only showed a 10 %
493 contribution to $\text{PM}_{2.5}$ mass. In addition, other previous studies (Yu et al., 2013; Zhang et al., 2013)
494 also reported significant contribution of soil dust to $\text{PM}_{2.5}$ mass, suggesting that soil dust is an
495 important contributor to $\text{PM}_{2.5}$ mass in the Beijing area. It is also expected as Beijing is in a semi-arid
496 region and there are sparsely vegetated surfaces both within and outside the city. This factor also
497 showed good agreement with the crustal fraction estimated from the element masses only during
498 winter at PG ($r^2=0.51$) and summer at IAP ($r^2=0.58$). This again highlights the probable mixing of
499 this source with other factors, or mis-attribution. Back trajectory analysis also indicates the influence
500 of regional transport during the summer period at IAP, dominated by south easterly-westerly flow
501 (Figure S9) due to high windspeeds (3.6 m s^{-1}). Therefore, there is a possibility that the high
502 contribution is linked to long-range transport in advected air masses. A recent study (Gu et al., 2020)
503 conducted in Beijing showed the high concentrations of more oxidised aerosols during summer due
504 to enhanced photochemical processes; however, such type of source was not resolved due to a lack
505 of filter based markers. This suggests the given source may contain some influence from an
506 unidentified/unresolved SOC fraction. Although the most plausible attribution appears to be to soil
507 dust, it is not fully resolved from other sources.

508
509 The use of Si in PMF could provide a better understanding on these dust related sources. However, it
510 is not used in the present PMF input due to high number of missing data points. The sensitivity of
511 PMF results to the use of Si has also been investigated by adding Si to the input matrix and providing
512 high uncertainty to the missing data. No change was observed in the factor profile and temporal
513 variation of the resolved factors compared to the present one. In addition, we also noticed a good
514 correlation between Si and Al, where Al has been used in PMF (Figure S10). Several PMF runs were

also made with inorganic data only, however the resolved factors were either mixed or hard to identify. In addition, attempts to improve the PMF results by varying the input species and by analysing data for the IAP and PG sites separately did not offer any advantage.

3.2 Comparison of Filter-Based PMF Results with other Receptor Modelling Approaches on the same Dataset

The source apportionment results from PMF were compared with those from CMB on the same filter-based composition data and PMF performed on other measurements (i.e. online AMS (PM_{10}), offline AMS ($PM_{2.5}$)) to get a deeper insight into the identified PMF factors and their origins (Figures 4, 5, 6, and 7). The CMB method resulted in the estimation of eight OC sources (i.e., vegetative detritus, residential coal combustion (CC), industrial CC, cooking, diesel vehicles, gasoline vehicles, biomass burning, other OC), including one secondary factor (Other OC) at both sites (IAP and PG) The online AMS datasets allowed the identification of 6 OA (MOOOA (more oxidised oxygenated OA), LOOOA (low more oxidised oxygenated OA), OPOA (oxidised primary OA), BBOA (biomass burning OA), COA (cooking OA), CCOA (coal combustion OA) factors during winter at IAP, while analyses on the offline AMS measurements resolved 4 OA (OOA, BBOA, COA, CCOA) factors.

For these analyses, OC concentrations related to the online/offline AMS OA factors were further calculated by applying OC-to-OA conversion factors specific to each source, i.e., 1.35 for coal combustion organic carbon (Sun et al., 2016), 1.38 for cooking organic carbon, 1.58 for biomass burning organic carbon (Xu et al., 2019), and 1.78 for the oxygenated fraction (Huang et al., 2010) and used to evaluate the OC concentrations of relevant OA factors.

Only OC equivalent concentrations were used to perform comparison for all approaches. OC mass closure was also verified at IAP during the wintertime by investigating the relation between: OC modelled by online AMS PMF vs filter based PMF ($r^2=0.7$, slope=1.17), OC measured vs OC

541 modelled by filter based PMF ($r^2=0.7$, slope=1.07), OC measured vs OC modelled by online AMS
 542 PMF ($r^2=0.9$, slope=0.92), OC modelled by offline AMS PMF vs OC model by filter based PMF
 543 ($r^2=0.6$, slope=0.75), OC measured vs OC modelled by offline AMS PMF ($r^2=0.9$, slope=1.41), and
 544 OC measured vs WSOA (offline AMS) ($r^2=0.9$, slope=0.85) (Figure S11). The comparison of OC
 545 modelled by PMF and CMB was also investigated at IAP ($r^2=0.8$, slope=1.05) and PG ($r^2=0.6$,
 546 slope=1.78) (Figure S12). All source apportionment approaches showed a fairly good agreement in
 547 reconstructing the total OC mass, justifying their direct comparison. In addition, it should be noted
 548 that the difference in the sampling size cut-off between online AMS (NR-PM₁) and filter
 549 measurements (PM_{2.5}) may contribute to the differences observed in the source apportionment
 550 results. Therefore, we also compared the relation between NR-PM measured vs PM measured
 551 ($r^2=0.96$, slope=0.92), and NR-PM measured vs PM modelled by filter based PMF ($r^2=0.9$,
 552 slope=1.29) (Figure S13). The agreements observed suggest that the most of the PM_{2.5} mass was
 553 accounted for by the PM₁ fraction, indicating that the difference in the size-cut off is relatively small.

554

555 (a) With CMB results at IAP

556 Resolved CMB and PMF factors were compared including data from both seasons at IAP and PG
 557 (Figure 4). A good correlation ($r^2=0.6$, $n=68$, $p<0.05$) was observed between biomass burning factors,
 558 suggesting that this source was well resolved using both approaches (Figure 4). However, a slightly
 559 higher concentration was reported by the CMB model (2.0 and 1.6 $\mu\text{g m}^{-3}$ by CMB and PMF
 560 respectively). Individual coal combustion factors (industrial/residential) did not show any
 561 significant correlation ($r^2<0.2$) with the coal combustion factor identified using PMF, although the
 562 total coal combustion fraction from CMB, the sum of industrial and residential fractions, did show
 563 an improved correlation ($r^2=0.4$). Some improvement on the correlation was seen if two outlier
 564 datapoints were removed (see Figure 4). A likely reason is that PMF did not resolve coal combustion
 565 and biomass burning factors well as both factors presented a strong seasonal pattern with high

566 concentrations during the winter. Another possibility is the difficulty in resolving primary and
567 secondary fractions due to a lack of secondary organic markers used in the study. This was further
568 supported by the fact noted above that the PMF biomass burning factor also contained some signal
569 from coal combustion activities. The sum of coal combustion and biomass burning factors from both
570 approaches showed a good correlation ($r^2=0.7$, $n=68$, $p<0.05$), suggesting a common emission pattern
571 (e.g., high in winter and low in summer), making it challenging to resolve them. Factors linked to
572 vehicle emissions did not show any correlation. A weak correlation ($r^2=0.3$, $n=68$, $p<0.05$) was
573 observed between Other OC from CMB, a proxy for the secondary organic fraction and the PMF
574 secondary inorganics factor. In addition, other OC also weakly correlated with soil dust ($r^2=0.22$,
575 $n=34$, $p<0.05$) in summer, suggesting the mixing of unresolved secondary fraction with soil dust
576 profile and supports the hypothesis discussed above. It should be noted that other OC could also
577 contain unresolved primary fractions as PMF results indicated substantial influence of industrial
578 emissions and dust related sources. However, the source profiles related to industrial emissions and
579 dust were not accounted for in the CMB model (Xu et al., ~~2020~~2021).

580

581 (b) With CMB results at PG

582 The comparison was also made using data from both seasons at PG (Figure 5). Biomass burning
583 aerosols showed a good correlation for both approaches ($r^2=0.7$, $n=20$, $p<0.05$) but a substantially
584 higher concentration was estimated by the CMB model ($5.1 \mu\text{g m}^{-3}$ and $2.0 \mu\text{g m}^{-3}$ by CMB and PMF
585 respectively). A significant correlation was also seen between traffic related factors from CMB and
586 PMF (gasoline-CMB vs traffic ($r^2=0.6$, $n=20$, $p<0.05$), diesel-CMB vs traffic ($r^2=0.6$, $n=20$, $p<0.05$)),
587 indicating that traffic sources resolved using PMF at the PG site may have included signals from both
588 diesel and gasoline vehicles; however it was not conclusive at the IAP site, as discussed above. This
589 suggests the traffic source resolved using PMF may contain particles linked to traffic emissions, but
590 the influence of other sources is prominent at IAP and resulted in poor correlation. In addition, for

591 traffic related factors from CMB, both showed a higher concentration (gasoline-CMB=0.8 $\mu\text{g m}^{-3}$,
 592 diesel-CMB=4.5 $\mu\text{g m}^{-3}$, traffic-PMF=0.2 $\mu\text{g m}^{-3}$). As with IAP, no significant correlation was
 593 observed between coal combustion factors from both approaches. The sum of coal combustion and
 594 biomass burning factors from both approaches also did not present a good correlation ($r^2=0.3$, $n=20$,
 595 $p<0.05$). This highlights the limitation of these methodologies to apportion sources when extreme
 596 meteorological conditions may lead to high internal mixing of sources. Unfavourable dispersion
 597 conditions have been previously observed in the Beijing region during severe haze events in winter
 598 (Wang et al., 2014). A high correlation was observed between Other OC (CMB) and secondary
 599 inorganics (PMF) ($r^2=0.7$, $n=20$, $p<0.05$). In addition, Other OC also showed a very high correlation
 600 with the biomass burning factor resolved from PMF ($r^2=0.9$, $n=20$, $p<0.05$). This suggests that the
 601 biomass burning factor in PMF may contain a substantial amount of aged aerosols since carbon
 602 emitted during biomass burning is in some cases oxygenated and water soluble (Lee et al.,
 603 ~~2008a~~[2008b](#)) and is subject to rapid oxidation in the atmosphere.
 604

605 **(c) With online AMS PMF factors at IAP (winter)**

606 BBOC (biomass burning OC) from PMF-AMS analysis agreed well with that from PMF ($r^2=0.7$,
 607 $n=27$, $p<0.05$; 4.0 $\mu\text{g m}^{-3}$ and 3.1 $\mu\text{g m}^{-3}$ by online AMS and PMF, respectively) (Figure 6). Coal
 608 combustion related factors showed a modest correlation (CCOC (coal combustion OC) vs coal
 609 combustion-PMF, $r^2=0.4$, $n=27$, $p<0.05$) but the mass concentration of the coal combustion source
 610 by PMF (11.3 $\mu\text{g m}^{-3}$) is significantly higher than by PMF-AMS (CCOC=4.7 $\mu\text{g m}^{-3}$). This may
 611 partly be due to the different size cut offs used by these measurements (PM_{10} for AMS vs $\text{PM}_{2.5}$). In
 612 addition, significant improvement on the correlation was seen if two outlying points were removed
 613 ($r^2=0.8$, see Figure 6). Oxygenated fractions from AMS, MOOOC (more oxidised oxygenated OC)
 614 and LOOOC (low oxidised oxygenated OC) also exhibited a good correlation with secondary
 615 inorganics (LOOOC vs secondary inorganics ($r^2=0.6$, $n=27$, $p<0.05$, LOOOC=2.9 $\mu\text{g m}^{-3}$, secondary
 616 inorganics=1.6 $\mu\text{g m}^{-3}$), MOOOC vs secondary inorganics ($r^2=0.7$, $n=27$, $p<0.05$, MOOOC=4.4 $\mu\text{g m}^{-3}$)).

617 m^{-3}). This was also confirmed by LOOOC and MOOOC showing a good correlation with NO_3^- and
618 SO_4^{2-} previously (Cao et al., 2017). The formation of both secondary inorganic aerosol and
619 oxygenated organic aerosol is dependent upon largely the same set of oxidant species, notably but
620 not solely the hydroxyl and nitrate radicals. In both cases there are also both homogeneous and
621 heterogeneous (aqueous phase) pathways, so conditions which promote the formation of oxidised
622 organic aerosol will also favour formation of secondary inorganic aerosol, and hence a correlation is
623 to be expected, and is often observed (Hu et al., 2016; Zhang et al., 2011).~~This suggests the~~
624 ~~oxygenated fractions from AMS and secondary inorganics are subject to similar controls in the~~
625 ~~atmosphere.~~ In addition, both oxygenated fractions were also found to be correlated with biomass
626 burning aerosols (LOOOC vs biomass burning-PMF ($r^2=0.7$, $n=27$, $p<0.05$), MOOOC vs biomass
627 burning-PMF ($r^2=0.6$, $n=27$, $p<0.05$)). This further highlights a potentially important role of biomass
628 burning activity in SOA formation at IAP. A good correlation was also observed between OPOC
629 (oxidised primary OC) and secondary inorganics and biomass burning ($r^2=0.7$, $n=27$, $p<0.05$).

630

631 (d) Offline AMS PMF factors at IAP (winter)

632 BBOC from PMF-offline AMS analysis showed a good correlation with that from PMF ($r^2=0.6$, $n=32$,
633 $p<0.05$) (Figure 7) but the mass concentration of BBOC ($4.6 \mu\text{g m}^{-3}$) is higher than biomass burning
634 ($3.1 \mu\text{g m}^{-3}$) from PMF. This was also noticed above while comparing with BBOC resolved using
635 online AMS PMF, suggesting a potential uncertainty in estimating the source contribution from
636 biomass burning. The uncertainty in filter-based PMF analysis could be related to model error. This
637 was further supported as biomass burning factor also made significant contributions to Ca^{2+} (15%),
638 Ni (30%), Cu (50%), and Al (35%), and these species are not necessarily from biomass burning
639 emissions but they were not resolved by PMF. In addition, the uncertainties linked to PMF-AMS
640 analysis could also contribute. A high correlation was noticed for secondary factors resolved using
641 both approaches (OOC (oxygenated OC) vs Secondary inorganics, $r^2=0.8$, $n=32$, $p<0.05$). OOC also
642 showed a good correlation with the biomass burning factor (OOC vs biomass burning-PMF, $r^2=0.7$,

643 n=32, $p<0.05$). This supports the hypothesis discussed previously on the origin of oxygenated
644 fractions.

645
646 Overall, the comparison of filter based PMF results was in broad agreement with other receptor
647 modelling approaches applied on the same dataset. However, large discrepancies were also observed
648 for some factors / sources. Common sources such as biomass burning and coal combustion were well
649 resolved using all approaches with some exceptions observed when using filter based PMF approach.
650 This could be linked to internal mixing of sources when the influence of climate and local
651 meteorology on both sources is predominant and making it challenging to resolve using PMF. A good
652 agreement was also observed between secondary inorganic aerosols and secondary fractions resolved
653 using other approaches. However, sources identified based on metal signatures using PMF indicated
654 some mixing or mis-attribution. For example, the influence of unresolved SOC on the soil dust profile
655 was observed during summer.

656

657 **3.3. Comparison with Previous PMF Source Apportionment Results in Beijing**

658 In this section an attempt has been made to understand the PM sources identified in the Beijing
659 metropolitan area by previous studies. The goal was here to assess the previous PMF source
660 apportionment results and report any discrepancies noticed in the resolved sources using PMF. This
661 may provide useful insight on sources resolved in the present study and also in exploring the issues
662 associated with filter based PMF modelling in the Beijing metropolitan area. Details of the studies
663 conducted to evaluate PM sources using a PMF model applied to inorganic and organic markers in
664 the Beijing metropolitan area are presented in Table [4-S5](#) and the major outcomes are discussed
665 hereafter.

666
667 Overall, these previous PMF studies provide insights on PM sources in the Beijing metropolitan area
668 (Li et al., 2019; Ma et al., 2017a; Tian et al., 2016; Yu et al., 2013; Song et al., 2007; Song et al.,

2006; Liu et al., 2019; Wang et al., 2008; Zhang et al., 2013). The major identified sources are dust, traffic emissions, coal combustion, industrial activity, secondary inorganic aerosols and biomass burning. Although there is a general issue of their inability to identify sources such as secondary organic aerosol and cooking emissions, similar to the present study, due to the lack of organic markers used in the PMF model to apportion these sources. However, beyond this, their PMF outcomes were not consistent. Large discrepancies between the sources were seen (Table [4S5](#)) based on the sources identified as well as their contribution to PM mass concentrations. Several factors could cause these differences such as the chemical species used as input in the PMF model, the period of the study, identification of sources based on chemical signatures and changes to the sources with time.

Input species considered within the previous studies were combinations of water-soluble ions, metallic elements, OC and EC. Similar input species were used in all of these studies, with the exception of the studies by Yu et al. (2013) and Li et al. (2019) who used only metallic elements for the source apportionment. As shown in this study, including organic markers may help to resolve some of the primary sources.

Another important parameter, the chemical species used for identifying sources were not always consistent. For example, coal combustion was resolved based on high contribution of OC, EC, and Cl present in the factor profile by Zhang et al. (2013), Wang et al. (2008), Song et al. (2007) and Song et al. (2006), in accordance with source profiles determined in the laboratory (Zheng et al., 2005). High Cl associated with fine aerosols in winter is a distinctive feature in Beijing and even around inland China, which is ascribed to coal combustion (Wang et al., 2008). Contrarily, Tian et al. (2016) identified coal combustion based on a high contribution of OC and EC, while the high contribution of Cl was attributed to a biomass burning source, similar to another study (Ma et al., 2017a). In other studies (Li et al., 2019; Yu et al., 2013; Liu et al., 2019) coal combustion was resolved based on the presence of metallic elements such as V, Se, Co, Cd, As and Ni, where V and Ni are widely used

695 markers for oil combustion (Mazzei et al., 2008). High loadings of As and Se have also been reported
696 as a typical source characteristic of coal combustion (Vejahati et al., 2010). Similar to coal
697 combustion, biomass burning was often characterised using the presence of K (Li et al., 2019; Tian
698 et al., 2016; Yu et al., 2013; Song et al., 2007; Song et al., 2006; Zhang et al., 2013; Liu et al., 2019;
699 Wang et al., 2008), a typical marker of biomass burning. Farming in Beijing's suburban districts has
700 been extensive in recent years. Burning of the crop remnants and fallen leaves by farmers in autumn
701 and winter results in the enhanced emissions of K. In addition, the contributions of Cl and Na were
702 also considered for the identification of these sources in some cases, depending on the species used
703 within the input (Song et al., 2007; Song et al., 2006; Tian et al., 2016). This highlights the fact that
704 none of the studies have used organic markers such as picene and levoglucosan which are very
705 specific to these combustion sources as discussed before, which may cause uncertainty in the resolved
706 sources. However, in the present study the use of organic markers played a key role in the
707 identification of these sources and their better apportionment. Despite this, some issues were observed
708 with these identified sources during winter due to extreme meteorological conditions as well as co-
709 emission of these aerosols at the same time, probably indicative of poor performance of the PMF
710 model under certain conditions.

711

712 Other important sources linked to traffic emissions, industrial activities and dust, are commonly
713 resolved among all the studies. The characterisation of these sources was predominantly based on the
714 metallic elements. For example, Zn, Cu, and Pb including sometimes EC were most often used to
715 characterise traffic emissions among all previous studies. Both Zn and Cu have been identified within
716 brake linings and tyre fragments (Thorpe and Harrison, 2008) and Pb has been used in the past within
717 gasoline as an anti-knock additive in China (Li et al., 2019). However, Cu and Zn can also serve as
718 indicators for industrial sources (Li et al., 2017; Yu et al., 2013). Other metallic elements (e.g., Sb,
719 Cr, Mn, K, Br and Ba) were also considered in certain cases to trace traffic emissions (Ma et al.,
720 2017a; Tian et al., 2016; Yu et al., 2013). However, a high contribution of Cr, Mn and sometimes Fe

721 to the given sources has also been attributed to industrial activities. Both Cr and Cr-containing
722 compounds are widely used in metallurgy, electroplating, pigment, leather and other industries
723 (Dall'Osto et al., 2013). A previous study found that ferrous metallurgy could emit Mn (Querol et al.,
724 2006). Furthermore, both Fe and Mn are characteristic components of iron and steel industry
725 emissions. In addition, Co, Mg, Al, Ca, Cd, Pb, Tl, Zn, V, Ni and Cu were also considered for the
726 apportionment of industrial sources (Tian et al., 2016; Yu et al., 2013). Zhang et al. (2013) identified
727 a mixed source of traffic and incineration emissions, based on high loading of Cu, Zn, Cd, Pb, Sb,
728 Sn, Mo, NO_3^- and EC. In the present study, the assignment of road traffic emissions was based on
729 high loadings of Zn and Pb. It was also seen that the given source may contain some influence from
730 industrial activities, as the industrial contribution was not resolved like previous studies and probably
731 accounted in other factors. Thus, it is clear that these metals could belong to several sources and their
732 proper assignment to respective sources is difficult in the complex environment.

733

734 The same issue was observed with the assignments of dust type (dust/road dust/soil dust/mineral
735 dust/yellow dust/local dust) sources. Although the dust type sources were often found to be composed
736 of crustal elements (e.g., Ca, Mg, Si, Ti, Al, Fe), the attribution of crustal elements to a particular
737 source was not consistent from one study to another previously. The two dust sources (road dust and
738 soil dust) identified in the present study also indicated mixing with other factors.

739

740 The identification of the secondary inorganic aerosol factors was often based on the high contribution
741 of water soluble ions (NO_3^- , SO_4^{2-} , NH_4^+), consistent with other studies (Ma et al., 2017a; Song et al.,
742 2007; Song et al., 2006; Tian et al., 2016; Liu et al., 2019; Wang et al., 2008; Zhang et al., 2013).
743 These results highlight the role of chemical species used in characterising source profiles and their
744 influence on the variability noticed in the Beijing metropolitan area. This issue arises because many
745 of these species are not source specific, making it challenging to directly link PMF factors to sources.
746 Pant and Harrison (2012), reviewing receptor modelling studies from India, noted a tendency to

747 attribute metal-rich source profiles to “industry” in a rather casual manner without evidence of local
748 industrial sources.

749
750 The change in sources and emissions over the course of time due to stringent emissions regulations
751 could also be considered plausible for the observed variability in the chemical profile and contribution
752 of identified sources. Li et al. (2019) showed levels of trace metals (V, Cr, Mn, As, Cd and Pb)
753 decreased more than 40% due to the emission regulations, while crustal elements decreased
754 considerably (4–45%), suggesting emissions from anthropogenic activities were suppressed. A
755 reduction in the contribution of sources such as dust and industrial activity was observed in the present
756 study and another recent study performed by Liu et al. (2019) relative to the previous ones, indicating
757 the effect of regulatory measures on the contribution of identified sources to PM_{2.5}. However, the
758 concentration of the majority of metallic elements (K, Cr, Mn, Fe, Co, Cu, Zn, As, Ag, Cd and Pb)
759 increased when pollution levels changed from clean days to heavily polluted days. This highlights
760 that specific atmospheric conditions could also play a major role for the observed variability. Another
761 factor is the time of year when these studies were conducted as some of the identified sources (e.g.,
762 coal combustion and biomass burning) exhibit typical seasonal patterns. During a low concentration
763 period, PMF models may have difficulty in resolving sources, leading to mixing of factors.

764
765 Overall, the present study provides a view of existing PM_{2.5} sources in the Beijing metropolitan area
766 by applying the PMF model to a filter-based dataset, which included water soluble ions, metals and
767 organic markers. Despite this, factors that were resolved based on metal signatures were not fully
768 resolved and indicate a mixing of different sources. As a part of same campaign, also discussed above,
769 Liu et al. (2019) used a similar approach by applying PMF on high resolution (1-hour) data, which
770 included OC, EC, ions, and metals, and did not encounter any issue. However, previous filter based
771 PMF studies conducted in the Beijing region that mostly included ions and metals in their input
772 dataset often showed difficulty in the proper assignment of metals to their respective sources. Even
773 the use of metal signatures from one to another study was not consistent. This highlights that the low

temporal resolution of filter data could not capture fast occurring atmospheric processes in Beijing, and may lead to a “blurring” of sources by the long averaging period. Atmospheric circulation and dynamic mechanisms play a key role in persistent haze events in Beijing during the cold period (Wu et al., 2017; Feng et al., 2014). Such events are associated with the high pollution periods and will offer opportunities for chemical and physical transformation within the aerosol that lead to contravention of the requirement of receptor models for preservation of chemical profiles between source and receptor.

781

782 4. CONCLUSION

This study presents the outcomes of PMF performed on the combined dataset collected at two sites (IAP and PG) in the Beijing metropolitan area, including their comparison with source apportionment results from other approaches or based on different measurements. The PMF analysis resulted in the identification of seven sources: coal combustion, biomass burning, oil combustion, secondary inorganics, traffic emissions, road dust and soil dust. These results were in a good agreement with previously published source apportionment results made using PMF. However, factors that were resolved based on metal signatures were not fully resolved and indicate an internal mixing of different sources. In particular, soil dust, road dust and some industrial sources have many elements in common and are very difficult to distinguish.

792

PMF results were compared with sources resolved from CMB and with PMF performed on other measurements (online AMS, offline AMS). Results showed a broad agreement with some notable exceptions. While this study provides some confirmatory evidence on PM_{2.5} source apportionment in Beijing, it highlights weaknesses of the PMF method when applied in this locality, and the results should be viewed in the context of studies using other methods such as CMB which appear able to give a more comprehensive view of the key sources affecting air quality. No industrial source profiles

799 were used as inputs to the CMB model reported here, so CMB offers no further insights into possible
800 contributions from industry.

801
802 **AUTHOR CONTRIBUTIONS**

803 This study was conceived by ZS and RMH. DS performed the PMF analysis and wrote the paper with
804 the help of Z.S. and R.M.H. T.V.V. and D.L. conducted the aerosol sampling and laboratory-based
805 chemical analyses. X.W. and J.X. conducted the CMB modelling at PG and IAP sites, respectively.
806 All authors discussed the paper and approved the final version for publication.

807
808 **COMPETING INTERESTS**

809 The authors declare that they have no conflict of interest.

810
811 **SPECIAL ISSUE STATEMENT**

812 This article is part of the special issue “In-depth study of air pollution sources and processes within
813 Beijing and its surrounding region (APHH-Beijing) (ACP/AMT inter-journal SI)”. It is not associated
814 with a conference.

815
816 **FINANCIAL SUPPORT**

817 This research has been supported by the Natural Environment Research Council (APHH and SOA
818 grants): NE/N007190/1 (AIRPOLL-Beijing), NE/S006699/1 (SOA).

819

820 REFERENCES

- 821 Amato, F., Pandolfi, M., Escrig, A., Querol, X., Alastuey, A., Pey, J., Perez, N., and Hopke, P. K.:
 822 Quantifying road dust resuspension in urban environment by Multilinear Engine: A comparison with
 823 PMF2, *Atmos. Environ.*, 43, 2770-2780, <https://doi.org/10.1016/j.atmosenv.2009.02.039>, 2009.
- 824
 825 Amato, F., and Hopke, P. K.: Source apportionment of the ambient PM_{2.5} across St. Louis using
 826 constrained positive matrix factorization, *Atmos. Environ.*, 46, 329-337,
 827 <https://doi.org/10.1016/j.atmosenv.2011.09.062>, 2012.
- 828
 829 Batterman, S., Xu, L., Chen, F., Chen, F., and Zhong, X.: Characteristics of PM_(2.5) Concentrations
 830 across Beijing during 2013-2015, *Atmos. Environ.* (Oxford, England: 1994), 145, 104-114,
 831 [10.1016/j.atmosenv.2016.08.060](https://doi.org/10.1016/j.atmosenv.2016.08.060), 2016.
- 832
 833 Bi, X., Simoneit, B. R. T., Sheng, G., and Fu, J.: Characterization of molecular markers in smoke
 834 from residential coal combustion in China, *Fuel*, 87, 112-119,
 835 <https://doi.org/10.1016/j.fuel.2007.03.047>, 2008.
- 836
 837 Boucher, O., Randall, D., Artaxo, P., Bretherton, C., Feingold, G., Forster, P., Kerminen, V.-M.,
 838 Kondo, Y., Liao, H., and Lohmann, U.: Clouds and aerosols, in: *Climate change 2013: the physical*
 839 *science basis. Contribution of Working Group I to the Fifth Assessment Report of the*
 840 *Intergovernmental Panel on Climate Change*, Cambridge University Press, 571-657, 2013.
- 841
 842 Cai, T., Zhang, Y., Fang, D., Shang, J., Zhang, Y., and Zhang, Y.: Chinese vehicle emissions
 843 characteristic testing with small sample size: Results and comparison, *Atmospheric Pollution*
 844 *Research*, 8, 154-163, <https://doi.org/10.1016/j.apr.2016.08.007>, 2017.
- 845
 846 Canepari, S., Perrino, C., Olivieri, F., and Astolfi, M. L.: Characterisation of the traffic sources of
 847 PM through size-segregated sampling, sequential leaching and ICP analysis, *Atmos. Environ.*, 42,
 848 8161-8175, <https://doi.org/10.1016/j.atmosenv.2008.07.052>, 2008.
- 849
 850 Cao, L., Zhu, Q., Huang, X., Deng, J., Chen, J., Hong, Y., Xu, L., and He, L.: Chemical
 851 characterization and source apportionment of atmospheric submicron particles on the western coast
 852 of Taiwan Strait, China, *J. Environ. Sci.*, 52, 293-304, <https://doi.org/10.1016/j.jes.2016.09.018>,
 853 2017.
- 854
 855 Chan, Y., Simpson, R., McTainsh, G., Vowles, P., Cohen, D., and Bailey, G. J. A. E.: Characterisation
 856 of chemical species in PM_{2.5} and PM₁₀ aerosols in Brisbane, Australia, *Atmos. Environ.*, 31, 3773-
 857 3785, 1997.
- 858
 859 Dall'Osto, M., Querol, X., Amato, F., Karanasiou, A., Lucarelli, F., Nava, S., Calzolari, G., and Chiari,
 860 M.: Hourly elemental concentrations in PM_{2.5} aerosols sampled simultaneously at urban background
 861 and road site during SAPUSS - diurnal variations and PMF receptor modelling, *Atmos. Chem. Phys.*,
 862 13, 4375, 2013.
- 863
 864 Draxler, R.: *Hysplit4 User's Guide*. NOAA Tech. Memo. ERL ARL-230, 35 pp.
 865 http://www.arl.noaa.gov/documents/reports/hysplit_user_guide.pdf, 1999.
- 866
 867 Duong, T. T. T., and Lee, B.-K.: Determining contamination level of heavy metals in road dust from
 868 busy traffic areas with different characteristics, *J. Environ. Manage.*, 92, 554-562,
 869 <https://doi.org/10.1016/j.jenvman.2010.09.010>, 2011.
- 870

- Duvall, R. M., Majestic, B. J., Shafer, M. M., Chuang, P. Y., Simoneit, B. R. T., and Schauer, J. J.: The water-soluble fraction of carbon, sulfur, and crustal elements in Asian aerosols and Asian soils, *Atmos. Environ.*, 42, 5872-5884, <https://doi.org/10.1016/j.atmosenv.2008.03.028>, 2008.
- Eglinton, G., Gonzalez, A. G., Hamilton, R. J., and Raphael, R. A.: Hydrocarbon constituents of the wax coatings of plant leaves: A taxonomic survey, *Phytochemistry*, 1, 89-102, [https://doi.org/10.1016/S0031-9422\(00\)88006-1](https://doi.org/10.1016/S0031-9422(00)88006-1), 1962.
- Feng, X., Li, Q., Zhu, Y., Wang, J., Liang, H., and Xu, R.: Formation and dominant factors of haze pollution over Beijing and its peripheral areas in winter, *Atmos. Pollut. Res.*, 5, 528-538, <https://doi.org/10.5094/APR.2014.062>, 2014.
- GBD MAPS Working Group: Burden of Disease Attributable to Coal-Burning and Other Major Sources of Air Pollution in China, Special Report 20, Health Effects Institute, Boston, MA, 2016.
- Grigoratos, T., and Martini, G.: Brake wear particle emissions: a review, *Environ. Sci. Pollut. Res.*, 22, 2491-2504, 10.1007/s11356-014-3696-8, 2015.
- Gu, Y., Huang, R.-J., Li, Y., Duan, J., Chen, Q., Hu, W., Zheng, Y., Lin, C., Ni, H., Dai, W., Cao, J., Liu, Q., Chen, Y., Chen, C., Ovadnevaite, J., Ceburnis, D., and O'Dowd, C.: Chemical nature and sources of fine particles in urban Beijing: Seasonality and formation mechanisms, *Environ. Intl.*, 140, 105732, <https://doi.org/10.1016/j.envint.2020.105732>, 2020.
- Guo, H., Zhou, J., Wang, L., Zhou, Y., Yuan, J., and Zhao, R.: Seasonal variations and sources of carboxylic acids in PM_{2.5} in Wuhan, China, *Aerosol Air. Qual. Res.*, 15, 517-528, 10.4209/aaqr.2014.02.0040, 2015.
- Harrison, R. M., Vu, T. V., Jafar, H., and Shi, Z.: More mileage in reducing urban air pollution from road traffic, *Environ. Int.*, 149, 106329, <https://doi.org/10.1016/j.envint.2020.106329>, 2021.
- He, G., Pan, Y., and Tanaka, T.: The short-term impacts of COVID-19 lockdown on urban air pollution in China, *Nature Sustainability*, 3, 1005-1011, 10.1038/s41893-020-0581-y, 2020.
- Heal, M. R., Kumar, P., and Harrison, R. M.: Particles, air quality, policy and health, *Chem. Soc. Rev.*, 41, 6606-6630, 2012.
- Henry, R., Norris, G. A., Vedantham, R., and Turner, J. R.: Source Region Identification Using Kernel Smoothing, *Environ. Sci. Technol.*, 43, 4090-4097, 10.1021/es8011723, 2009.
- Herrera Murillo, J., Campos Ramos, A., Ángeles García, F., Blanco Jiménez, S., Cárdenas, B., and Mizohata, A.: Chemical composition of PM_{2.5} particles in Salamanca, Guanajuato Mexico: Source apportionment with receptor models, *Atmos. Res.*, 107, 31-41, 10.1016/j.atmosres.2011.12.010, 2012.
- Hopke, P. K.: Review of receptor modeling methods for source apportionment, *JAWMA*, 66, 237-259, 10.1080/10962247.2016.1140693, 2016.
- Hu, W., Hu, M., Hu, W., Jimenez, J. L., Yuan, B., Chen, W., Wang, M., Wu, Y., Chen, C., Wang, Z., Peng, J., Zeng, L., and Shao, M.: Chemical composition, sources, and aging process of submicron aerosols in Beijing: Contrast between summer and winter, 121, 1955-1977, 10.1002/2015jd024020, 2016.

923 Huang, X., Tang, G., Zhang, J., Liu, B., Liu, C., Zhang, J., Cong, L., Cheng, M., Yan, G., Gao, W.,
 924 Wang, Y., and Wang, Y.: Characteristics of PM_{2.5} pollution in Beijing after the improvement of air
 925 quality, *J. Environ. Sci.*, 100, 1-10, <https://doi.org/10.1016/j.jes.2020.06.004>, 2021.

926

927 Huang, X. F., He, L. Y., Hu, M., Canagaratna, M. R., Sun, Y., Zhang, Q., Zhu, T., Xue, L., Zeng, L.
 928 W., Liu, X. G., Zhang, Y. H., Jayne, J. T., Ng, N. L., and Worsnop, D. R.: Highly time-resolved
 929 chemical characterization of atmospheric submicron particles during 2008 Beijing Olympic Games
 930 using an Aerodyne High-Resolution Aerosol Mass Spectrometer, *Atmos. Chem. Phys.*, 10, 8933-
 931 8945, 10.5194/acp-10-8933-2010, 2010a.

932

933 ~~Huang, X. F., He, L. Y., Hu, M., Canagaratna, M. R., Sun, Y., Zhang, Q., Zhu, T., Xue, L., Zeng, L.~~
 934 ~~W., Liu, X. G., Zhang, Y. H., Jayne, J. T., Ng, N. L., and Worsnop, D. R.: Highly time-resolved~~
 935 ~~chemical characterization of atmospheric submicron particles during 2008 Beijing Olympic Games~~
 936 ~~using an Aerodyne High-Resolution Aerosol Mass Spectrometer, *Atmos. Chem. Phys.*, 10, 8933-~~
 937 ~~8945, 10.5194/acp-10-8933-2010, 2010b.~~

938

939 Jaekels, J. M., Bae, M.-S., and Schauer, J. J.: Positive matrix factorization (PMF) analysis of
 940 molecular marker measurements to quantify the sources of organic aerosols, *Environ. Sci. Technol.*,
 941 41, 5763-5769, 2007.

942

943 Ji, D., Li, L., Wang, Y., Zhang, J., Cheng, M., Sun, Y., Liu, Z., Wang, L., Tang, G., and Hu, B. J. A.
 944 E.: The heaviest particulate air-pollution episodes occurred in northern China in January, 2013:
 945 Insights gained from observation, *Atmos. Environ.*, 92, 546-556,
 946 doi.org/10.1016/j.atmosenv.2014.04.048, 2014.

947

948 Jing, B., Wu, L., Mao, H., Gong, S., He, J., Zou, C., Song, G., Li, X., and Wu, Z.: Development of a
 949 vehicle emission inventory with high temporal-spatial resolution based on NRT traffic data and its
 950 impact on air pollution in Beijing – Part 1: Development and evaluation of vehicle emission
 951 inventory, *Atmos. Chem. Phys.*, 16, 3161-3170, 10.5194/acp-16-3161-2016, 2016.

952

953 Kim, E.-A., and Koh, B.: Utilization of road dust chemical profiles for source identification and
 954 human health impact assessment, *Sci. Rep.*, 10, 14259, 10.1038/s41598-020-71180-x, 2020.

955

956 Kolattukudy, P. E.: Chemistry and biochemistry of natural waxes, Elsevier Scientific Pub. Co., 1976.

957

958 Laing, J. R., Hopke, P. K., Hopke, E. F., Husain, L., Dutkiewicz, V. A., Paatero, J., and Viisanen, Y.:
 959 Positive Matrix Factorization of 47 Years of Particle Measurements in Finnish Arctic, *Aerosol. Air*
 960 *Qual. Res.*, 15, 188-207 2015.

961

962 Le, T., Wang, Y., Liu, L., Yang, J., Yung, Y. L., Li, G., and Seinfeld, J. H.: Unexpected air pollution
 963 with marked emission reductions during the COVID-19 outbreak in China, *Science*, 369, 702,
 964 10.1126/science.abb7431, 2020.

965

966 Lee, B.-K., Hieu, N. T. J. A., and Resarch, A. Q.: Seasonal variation and sources of heavy metals in
 967 atmospheric aerosols in a residential area of Ulsan, Korea, 11, 679-688, 2011.

968

969 Lee, S., Liu, W., Wang, Y., Russell, A. G., and Edgerton, E. S.: Source apportionment of PM 2.5:
 970 Comparing PMF and CMB results for four ambient monitoring sites in the southeastern United States,
 971 *Atmos. Environ.*, 42, 4126-4137, 2008b2008a.

972

973 Lee, S., Kim, H. K., Yan, B., Cobb, C. E., Hennigan, C., Nichols, S., Chamber, M., Edgerton, E. S.,
 974 Jansen, J. J., Hu, Y., Zheng, M., Weber, R. J., and Russell, A. G.: Diagnosis of Aged Prescribed

975 Burning Plumes Impacting an Urban Area, *Environ. Sci. Technol.*, 42, 1438-1444,
976 10.1021/es7023059, ~~2008a~~2008b.
977

978 Li, M., Liu, Z., Chen, J., Huang, X., Liu, J., Xie, Y., Hu, B., Xu, Z., Zhang, Y., and Wang, Y.:
979 Characteristics and source apportionment of metallic elements in PM_{2.5} at urban and suburban sites
980 in Beijing: Implication of emission reduction, 10, 105, 2019.
981

982 Li, D., Liu, J., Zhang, J., Gui, H., Du, P., Yu, T., Wang, J., Lu, Y., Liu, W., and Cheng, Y.:
983 Identification of long-range transport pathways and potential sources of PM(2.5) and PM(10) in
984 Beijing from 2014 to 2015, *J. Environ. Sci. (China)*, 56, 214-229, 10.1016/j.jes.2016.06.035, 2017.
985

986 Lim, J.-M., Lee, J.-H., Moon, J.-H., Chung, Y.-S., and Kim, K.-H.: Source apportionment of PM₁₀ at
987 a small industrial area using Positive Matrix Factorization, *Atmos. Res.*, 95, 88-100,
988 <https://doi.org/10.1016/j.atmosres.2009.08.009>, 2010.
989

990 Liu, Y., Zheng, M., Yu, M., Cai, X., Du, H., Li, J., Zhou, T., Yan, C., Wang, X., Shi, Z., Harrison, R.
991 M., Zhang, Q., and He, K.: High-time-resolution source apportionment of PM_{2.5} in Beijing with
992 multiple models, *Atmos. Chem. Phys.*, 19, 6595-6609, 10.5194/acp-19-6595-2019, 2019.
993

994 Lu, X., Yuan, D., Chen, Y., and Fung, J. C. H.: Impacts of urbanization and long-term meteorological
995 variations on global PM_{2.5} and its associated health burden, *Environ. Pollut.*, 270, 116003,
996 <https://doi.org/10.1016/j.envpol.2020.116003>, 2021.
997

998 Ma, Q., Wu, Y., Tao, J., Xia, Y., Liu, X., Zhang, D., Han, Z., Zhang, X., and Zhang, R.: Variations
999 of Chemical composition and source apportionment of PM_{2.5} during winter haze episodes in Beijing,
1000 *Aerosol. Air Qual. Res.*, 17, 2791-2803, 10.4209/aaqr.2017.10.0366, 2017a.
1001

1002 Ma, Q., Wu, Y., Zhang, D., Wang, X., Xia, Y., Liu, X., Tian, P., Han, Z., Xia, X., Wang, Y., and
1003 Zhang, R.: Roles of regional transport and heterogeneous reactions in the PM_{2.5} increase during winter
1004 haze episodes in Beijing, *Sci. Tot. Environ.*, 599-600, 246-253,
1005 <https://doi.org/10.1016/j.scitotenv.2017.04.193>, 2017b.
1006

1007 Mazzei, F., D'Alessandro, A., Lucarelli, F., Nava, S., Prati, P., Valli, G., and Vecchi, R.:
1008 Characterization of particulate matter sources in an urban environment, *Sci. Tot. Environ.*, 401, 81-
1009 89, <https://doi.org/10.1016/j.scitotenv.2008.03.008>, 2008.
1010

1011 Niu, H., Hu, W., Zhang, D., Wu, Z., Guo, S., Pian, W., Cheng, W., and Hu, M.: Variations of fine
1012 particle physiochemical properties during a heavy haze episode in the winter of Beijing, *Sci. Tot.*
1013 *Environ.*, 571, 103-109, <https://doi.org/10.1016/j.scitotenv.2016.07.147>, 2016.
1014

1015 Norris, G., Duvall, R., Brown, S., and Bai, S.: EPA Positive Matrix Factorization (PMF) 5.0
1016 fundamentals and User Guide Prepared for the US Environmental Protection Agency Office of
1017 Research and Development, Washington, DC, DC EPA/600/R-14/108, 2014.
1018

1019 Oros, D. R., and Simoneit, B. R. T.: Identification and emission rates of molecular tracers in coal
1020 smoke particulate matter, *Fuel*, 79, 515-536, [https://doi.org/10.1016/S0016-2361\(99\)00153-2](https://doi.org/10.1016/S0016-2361(99)00153-2), 2000.
1021

1022 Paatero, P., and Hopke, P. K.: Discarding or downweighting high-noise variables in factor analytic
1023 models, *Anal. Chim. Acta*, 490, 277-289, 2003.
1024

1025 Paatero, P.: Least squares formulation of robust non-negative factor analysis, *Chemom. Intell. Lab.*
1026 *Syst.*, 37, 23-35, [http://doi.org/10.1016/S0169-7439\(96\)00044-5](http://doi.org/10.1016/S0169-7439(96)00044-5), 1997.

- Paatero, P., and Tapper, U.: Positive matrix factorization: A non-negative factor model with optimal utilization of error estimates of data values, *Environmetrics*, 5, 111-126, 1994.
- ~~Pacyna, J. M., and Pacyna, E. G.: An assessment of global and regional emissions of trace metals to the atmosphere from anthropogenic sources worldwide, *Environ. Rev.*, 9, 269-298, 10.1139/a01-012, 2001.~~
- Pant, P., Shukla, A., Kohl, S. D., Chow, J. C., Watson, J. G., and Harrison, R. M.: Characterization of ambient PM_{2.5} at a pollution hotspot in New Delhi, India and inference of sources, *Atmos. Environ.*, 109, 178-189, <http://dx.doi.org/10.1016/j.atmosenv.2015.02.074>, 2015.
- Pant, P., and Harrison, R. M.: Estimation of the contribution of road traffic emissions to particulate matter concentrations from field measurements: A review, *Atmos. Environ.*, 77, 78-97, <https://doi.org/10.1016/j.atmosenv.2013.04.028>, 2013.
- Pant, P., and Harrison, R. M.: Critical review of receptor modelling for particulate matter: a case study of India, *Atmos. Environ.*, 49, 1-12, 2012.
- Paraskevopoulou, D., Liakakou, E., Gerasopoulos, E., Theodosi, C., and Mihalopoulos, N.: Long-term characterization of organic and elemental carbon in the PM_{2.5} fraction: the case of Athens, Greece, *Atmos. Chem. Phys.*, 14, 13313-13325, 10.5194/acp-14-13313-2014, 2014.
- Paulot, F., Paynter, D., Ginoux, P., Naik, V., Whitburn, S., Van Damme, M., Clarisse, L., Coheur, P.-F., and Horowitz, L. W.: Gas-aerosol partitioning of ammonia in biomass burning plumes: Implications for the interpretation of spaceborne observations of ammonia and the radiative forcing of ammonium nitrate, 44, 8084-8093, <https://doi.org/10.1002/2017GL074215>, 2017.
- Petit, J. E., Favez, O., Albinet, A., and Canonaco, F.: A user-friendly tool for comprehensive evaluation of the geographical origins of atmospheric pollution: Wind and trajectory analyses, *Environ. Modell. Softw.*, 88, 183-187, <https://doi.org/10.1016/j.envsoft.2016.11.022>, 2017.
- Piscitello, A., Bianco, C., Casasso, A., and Sethi, R.: Non-exhaust traffic emissions: Sources, characterization, and mitigation measures, *Sci. Total Environ.*, 766, 144440, <https://doi.org/10.1016/j.scitotenv.2020.144440>, 2021.
- Polissar, A. V., Hopke, P. K., and Poirot, R. L.: Atmospheric aerosol over Vermont: chemical composition and sources, *Environ. Sci. Technol.*, 35, 4604-4621, 2001.
- Polissar, A. V., Hopke, P. K., Paatero, P., Malm, W. C., and Sisler, J. F.: Atmospheric aerosol over Alaska: 2. Elemental composition and sources, *J. Geophys. Res.-Atmos.*, 103, 19045-19057, 1998.
- Qiu, Y., Xie, Q., Wang, J., Xu, W., Li, L., Wang, Q., Zhao, J., Chen, Y., Chen, Y., Wu, Y., Du, W., Zhou, W., Lee, J., Zhao, C., Ge, X., Fu, P., Wang, Z., Worsnop, D. R., and Sun, Y.: Vertical Characterization and Source Apportionment of Water-Soluble Organic Aerosol with High-resolution Aerosol Mass Spectrometry in Beijing, China, *ACS Earth Space Chem.*, 3, 273-284, 10.1021/acsearthspacechem.8b00155, 2019.
- Querol, X., Zhuang, X., Alastuey, A., Viana, M., Lv, W., Wang, Y., López, A., Zhu, Z., Wei, H., and Xu, S.: Speciation and sources of atmospheric aerosols in a highly industrialised emerging mega-city in Central China, *J. Environ. Monit.*, 8, 1049-1059, 10.1039/B608768J, 2006.

1078 Rogge, W. F., Hildemann, L. M., Mazurek, M. A., Cass, G. R., and Simoneit, B. R. T.: Sources of
 1079 fine organic aerosol. 4. Particulate abrasion products from leaf surfaces of urban plants, *Environ. Sci.*
 1080 *Technol.*, 27, 2700-2711, 10.1021/es00049a008, 1993.

1081

1082 Schembari, C., Bove, M. C., Cuccia, E., Cavalli, F., Hjorth, J., Massabò, D., Nava, S., Udisti, R., and
 1083 Prati, P.: Source apportionment of PM₁₀ in the Western Mediterranean based on observations from a
 1084 cruise ship, *Atmos. Environ.*, 98, 510-518, 10.1016/j.atmosenv.2014.09.015, 2014.

1085

1086 Shi, Z., Song, C., Liu, B., Lu, G., Xu, J., Van Vu, T., Elliott, R. J. R., Li, W., Bloss, W. J., and
 1087 Harrison, R. M.: Abrupt but smaller than expected changes in surface air quality attributable to
 1088 COVID-19 lockdowns, *Sci. Adv.*, 7, 10.1126/sciadv.abd6696, 2021.

1089

1090 Shi, Z., Vu, T., Kotthaus, S., Harrison, R. M., Grimmond, S., Yue, S., Zhu, T., Lee, J., Han, Y.,
 1091 Demuzere, M., Dunmore, R. E., Ren, L., Liu, D., Wang, Y., Wild, O., Allan, J., Acton, W. J., Barlow,
 1092 J., Barratt, B., Beddows, D., Bloss, W. J., Calzolari, G., Carruthers, D., Carslaw, D. C., Chan, Q.,
 1093 Chatzidiakou, L., Chen, Y., Crilley, L., Coe, H., Dai, T., Doherty, R., Duan, F., Fu, P., Ge, B., Ge,
 1094 M., Guan, D., Hamilton, J. F., He, K., Heal, M., Heard, D., Hewitt, C. N., Hollaway, M., Hu, M., Ji,
 1095 D., Jiang, X., Jones, R., Kalberer, M., Kelly, F. J., Kramer, L., Langford, B., Lin, C., Lewis, A. C.,
 1096 Li, J., Li, W., Liu, H., Liu, J., Loh, M., Lu, K., Lucarelli, F., Mann, G., McFiggans, G., Miller, M. R.,
 1097 Mills, G., Monk, P., Nemitz, E., O'Connor, F., Ouyang, B., Palmer, P. I., Percival, C., Popoola, O.,
 1098 Reeves, C., Rickard, A. R., Shao, L., Shi, G., Spracklen, D., Stevenson, D., Sun, Y., Sun, Z., Tao, S.,
 1099 Tong, S., Wang, Q., Wang, W., Wang, X., Wang, X., Wang, Z., Wei, L., Whalley, L., Wu, X., Wu,
 1100 Z., Xie, P., Yang, F., Zhang, Q., Zhang, Y., Zhang, Y., and Zheng, M.: Introduction to the special
 1101 issue "In-depth study of air pollution sources and processes within Beijing and its surrounding region
 1102 (APHH-Beijing)", *Atmos. Chem. Phys.*, 19, 7519-7546, 10.5194/acp-19-7519-2019, 2019.

1103

1104 Shrivastava, M. K., Subramanian, R., Rogge, W. F., and Robinson, A. L.: Sources of organic aerosol:
 1105 Positive matrix factorization of molecular marker data and comparison of results from different
 1106 source apportionment models, *Atmos. Environ.*, 41, 9353-9369, 10.1016/j.atmosenv.2007.09.016,
 1107 2007.

1108

1109 Simoneit, B. R.: A review of biomarker compounds as source indicators and tracers for air pollution,
 1110 *Environ. Sci. Pollut. Res.*, 6, 159-169, 1999.

1111

1112 Smichowski, P., Gómez, D., Frazzoli, C., and Caroli, S.: Traffic-Related Elements in Airborne
 1113 Particulate Matter, *Applied Spectroscopy Reviews*, 43, 23-49, 10.1080/05704920701645886, 2007.

1114

1115 Song, Y., Tang, X., Xie, S., Zhang, Y., Wei, Y., Zhang, M., Zeng, L., and Lu, S.: Source
 1116 apportionment of PM_{2.5} in Beijing in 2004, *J. Hazard. Mater.*, 146, 124-130,
 1117 <https://doi.org/10.1016/j.jhazmat.2006.11.058>, 2007.

1118

1119 Song, Y., Zhang, Y., Xie, S., Zeng, L., Zheng, M., Salmon, L. G., Shao, M., and Slanina, S.: Source
 1120 apportionment of PM_{2.5} in Beijing by positive matrix factorization, *Atmos. Environ.*, 40, 1526-1537,
 1121 10.1016/j.atmosenv.2005.10.039, 2006.

1122

1123 Sörme, L., Bergbäck, B., and Lohm, U.: Goods in the Anthroposphere as a Metal Emission Source A
 1124 Case Study of Stockholm, Sweden, *Water, Air & Soil Pollut.: Focus*, 1, 213-227,
 1125 10.1023/A:1017516523915, 2001.

1126

1127 Srimuruganandam, B., and Shiva Nagendra, S. M.: Application of positive matrix factorization in
 1128 characterization of PM₁₀ and PM_{2.5} emission sources at urban roadside, *Chemosphere*, 88, 120-130,
 1129 <http://doi.org/10.1016/j.chemosphere.2012.02.083>, 2012.

1130
1131 Srivastava, D., Tomaz, S., Favez, O., Lanzafame, G. M., Golly, B., Besombes, J. L., Alleman, L. Y.,
1132 Jaffrezo, J. L., Jacob, V., Perraudin, E., Villenave, E., and Albinet, A.: Speciation of organic fraction
1133 does matter for source apportionment. Part 1: A one-year campaign in Grenoble (France), *Sci. Tot.*
1134 *Environ.*, 624, 1598-1611, 10.1016/j.scitotenv.2017.12.135, 2018.

1135
1136 Stein, A. F., Draxler, R. R., Rolph, G. D., Stunder, B. J. B., Cohen, M. D., and Ngan, F.: NOAA's
1137 HYSPLIT Atmospheric Transport and Dispersion Modeling System, *Bull. Am. Meteorol. Soc.*, 96,
1138 2059-2077, 10.1175/bams-d-14-00110.1, 2015.

1139
1140 Sun, Y., He, Y., Kuang, Y., Xu, W., Song, S., Ma, N., Tao, J., Cheng, P., Wu, C., Su, H., Cheng, Y.,
1141 Xie, C., Chen, C., Lei, L., Qiu, Y., Fu, P., Croteau, P., and Worsnop, D. R.: Chemical differences
1142 between PM₁ and PM_{2.5} in Highly polluted environment and implications in air pollution studies,
1143 *Geophys. Res. Lett.*, 47, e2019GL086288, 10.1029/2019GL086288, 2020.

1144
1145 Sun, Y., Du, W., Fu, P., Wang, Q., Li, J., Ge, X., Zhang, Q., Zhu, C., Ren, L., Xu, W., Zhao, J., Han,
1146 T., Worsnop, D. R., and Wang, Z.: Primary and secondary aerosols in Beijing in winter: sources,
1147 variations and processes, *Atmos. Chem. Phys.*, 16, 8309-8329, 10.5194/acp-16-8309-2016, 2016.

1148
1149 Sun, Y., Jiang, Q., Wang, Z., Fu, P., Li, J., Yang, T., and Yin, Y.: Investigation of the sources and
1150 evolution processes of severe haze pollution in Beijing in January 2013, 119, 4380-4398,
1151 <https://doi.org/10.1002/2014JD021641>, 2014.

1152
1153 Sun, Y. L., Wang, Z. F., Fu, P. Q., Yang, T., Jiang, Q., Dong, H. B., Li, J., and Jia, J. J.: Aerosol
1154 composition, sources and processes during wintertime in Beijing, China, *Atmos. Chem. Phys.*, 13,
1155 4577-4592, 10.5194/acp-13-4577-2013, 2013.

1156
1157 Sun, J., Zhang, Q., Canagaratna, M. R., Zhang, Y., Ng, N. L., Sun, Y., Jayne, J. T., Zhang, X., Zhang,
1158 X., and Worsnop, D. R.: Highly time- and size-resolved characterization of submicron aerosol
1159 particles in Beijing using an Aerodyne Aerosol Mass Spectrometer, *Atmos. Environ.*, 44, 131-140,
1160 <https://doi.org/10.1016/j.atmosenv.2009.03.020>, 2010.

1161
1162 Sun, Y., Zhuang, G., Tang, A., Wang, Y., and An, Z.: Chemical Characteristics of PM_{2.5} and PM₁₀
1163 in Haze–Fog Episodes in Beijing, *Environ. Sci. Technol.*, 40, 3148-3155, 10.1021/es051533g, 2006.

1164
1165 Sun, Y., Zhuang, G., Wang, Y., Zhao, X., Li, J., Wang, Z., and An, Z.: Chemical composition of dust
1166 storms in Beijing and implications for the mixing of mineral aerosol with pollution aerosol on the
1167 pathway, *J. Geophys. Chem.*, 110, D24209, 10.1029/2005jd006054, 2005.

1168
1169 Swietlicki, E., and Krejci, R.: Source characterisation of the Central European atmospheric aerosol
1170 using multivariate statistical methods, *Nucl. Instrum. Methods Phys. Res., Sect. B*, 109-110, 519-525,
1171 [https://doi.org/10.1016/0168-583X\(95\)01220-6](https://doi.org/10.1016/0168-583X(95)01220-6), 1996.

1172
1173 Takuwa, T., Mkilaha, I. S. N., and Naruse, I.: Mechanisms of fine particulates formation with alkali
1174 metal compounds during coal combustion, *Fuel*, 85, 671–678, 2006.

1175
1176 Tao, S., Ru, M. Y., Du, W., Zhu, X., Zhong, Q. R., Li, B. G., Shen, G. F., Pan, X. L., Meng, W. J.,
1177 Chen, Y. L., Shen, H. Z., Lin, N., Su, S., Zhuo, S. J., Huang, T. B., Xu, Y., Yun, X., Liu, J. F., Wang,
1178 X. L., Liu, W. X., Chen, H. F., and Zhu, D. Q.: Quantifying the Rural Residential Energy Transition
1179 in China from 1992 to 2012 through a Representative National Survey, *Nat. Energy*, 3, 567–573,
1180 2018.

1181

1182 Thorpe, A., and Harrison, R. M.: Sources and properties of non-exhaust particulate matter from road
 1183 traffic: A review, *Sci. Tot. Environ.*, 400, 270-282, <https://doi.org/10.1016/j.scitotenv.2008.06.007>,
 1184 2008.

1185

1186 Tian, S. L., Pan, Y. P., and Wang, Y. S.: Size-resolved source apportionment of particulate matter in
 1187 urban Beijing during haze and non-haze episodes, *Atmos. Chem. Phys.*, 16, 1-19, 10.5194/acp-16-1-
 1188 2016, 2016.

1189

1190 Tie, X., Huang, R.-J., Cao, J., Zhang, Q., Cheng, Y., Su, H., Chang, D., Pöschl, U., Hoffmann, T.,
 1191 Dusek, U., Li, G., Worsnop, D. R., and O'Dowd, C. D.: Severe Pollution in China Amplified by
 1192 Atmospheric Moisture, *Sci. Rep.*, 7, 15760-15760, 10.1038/s41598-017-15909-1, 2017.

1193

1194 Vejahati, F., Xu, Z., and Gupta, R.: Trace elements in coal: Associations with coal and minerals and
 1195 their behavior during coal utilization – A review, *Fuel*, 89, 904-911,
 1196 <https://doi.org/10.1016/j.fuel.2009.06.013>, 2010.

1197

1198 Viana, M., Kuhlbusch, T. A. J., Querol, X., Alastuey, A., Harrison, R. M., Hopke, P. K., Winiwarter,
 1199 W., Vallius, M., Szidat, S., Prévôt, A. S. H., Hueglin, C., Bloemen, H., Wählin, P., Vecchi, R.,
 1200 Miranda, A. I., Kasper-Giebl, A., Maenhaut, W., and Hitzenberger, R.: Source apportionment of
 1201 particulate matter in Europe: A review of methods and results, *J. Aerosol Sci.*, 39, 827-849,
 1202 <http://dx.doi.org/10.1016/j.jaerosci.2008.05.007>, 2008.

1203

1204 Vu, T. V., Shi, Z., Cheng, J., Zhang, Q., He, K., Wang, S., and Harrison, R. M.: Assessing the impact
 1205 of clean air action on air quality trends in Beijing using a machine learning technique, *Atmos. Chem.*
 1206 *Phys.*, 19, 11303-11314, 10.5194/acp-19-11303-2019, 2019.

1207

1208 Waked, A., Favez, O., Alleman, L. Y., Piot, C., Petit, J. E., Delaunay, T., Verlinden, E., Golly, B.,
 1209 Besombes, J. L., Jaffrezo, J. L., and Leoz-Garziandia, E.: Source apportionment of PM₁₀ in a north-
 1210 western Europe regional urban background site (Lens, France) using positive matrix factorization and
 1211 including primary biogenic emissions, *Atmos. Chem. Phys.*, 14, 3325-3346, 10.5194/acp-14-3325-
 1212 2014, 2014.

1213

1214 Wang, G., Gu, S., Chen, J., Wu, X., and Yu, J.: Assessment of health and economic effects by PM_{2.5}
 1215 pollution in Beijing: a combined exposure–response and computable general equilibrium analysis,
 1216 *Environ. Technol.*, 37, 3131-3138, 10.1080/09593330.2016.1178332, 2016.

1217

1218

1219 Wang, L., Zhang, N., Liu, Z., Sun, Y., Ji, D., and Wang, Y.: The Influence of Climate Factors,
 1220 Meteorological Conditions, and boundary-layer structure on severe haze pollution in the Beijing-
 1221 Tianjin-Hebei region during January 2013, *Adv. Meteorol.*, 2014, 685971, 10.1155/2014/685971,
 1222 2014.

1223

1224 Wang, Y., Hopke, P. K., Xia, X., Rattigan, O. V., Chalupa, D. C., and Utell, M. J.: Source
 1225 apportionment of airborne particulate matter using inorganic and organic species as tracers, *Atmos.*
 1226 *Environ.*, 55, 525-532, 2012.

1227

1228 Wang, Q., Shao, M., Zhang, Y., Wei, Y., Hu, M., and Guo, S.: Source apportionment of fine organic
 1229 aerosols in Beijing, *Atmos. Chem. Phys.*, 9, 8573-8585, 10.5194/acp-9-8573-2009, 2009.

1230

1231 Wang, H., Zhuang, Y., Wang, Y., Sun, Y., Yuan, H., Zhuang, G., and Hao, Z.: Long-term monitoring
 1232 and source apportionment of PM_{2.5}/PM₁₀ in Beijing, China, *J. Environ. Sci.*, 20, 1323-1327,
 1233 [https://doi.org/10.1016/S1001-0742\(08\)62228-7](https://doi.org/10.1016/S1001-0742(08)62228-7), 2008.

1234

1235 Watson, J. G., Robinson, N. F., Chow, J. C., Henry, R. C., Kim, B., Pace, T., Meyer, E. L., and
 1236 Nguyen, Q.: The USEPA/DRI chemical mass balance receptor model, CMB 7.0, *Environ. Soft.*, 5,
 1237 38-49, 1990.

1238

1239 Wu, X., Chen, C., Vu, T. V., Liu, D., Baldo, C., Shen, X., Zhang, Q., Cen, K., Zheng, M., He, K.,
 1240 Shi, Z., and Harrison, R. M.: Source apportionment of fine organic carbon (OC) using receptor
 1241 modelling at a rural site of Beijing: Insight into seasonal and diurnal variation of source contributions,
 1242 *Environ. Pollut.*, 115078, 2020.

1243

1244 Wu, P., Ding, Y., and Liu, Y. J. A. i. A. S.: Atmospheric circulation and dynamic mechanism for
 1245 persistent haze events in the Beijing–Tianjin–Hebei region, *Adv. Atmos. Sci.*, 34, 429-440, 2017.

1246

1247 Xie, Y., Dai, H., Zhang, Y., Wu, Y., Hanaoka, T., and Masui, T. J. E. i.: Comparison of health and
 1248 economic impacts of PM_{2.5} and ozone pollution in China, *Environ. Int.*, 130, 104881,
 1249 <https://doi.org/10.1016/j.envint.2019.05.075>, 2019.

1250

1251 Xing, Y.-F., Xu, Y.-H., Shi, M.-H., and Lian, Y.-X.: The impact of PM_{2.5} on the human respiratory
 1252 system, *J. Thorac. Dis.*, 8, E69-E74, 10.3978/j.issn.2072-1439.2016.01.19, 2016.

1253

1254 Xu, J., Liu, D., Wu, X., Vu, T., V., Zhang, Y., Fu, P., Sun, Y., Harrison, R., M., and Shi, Z.: Source
 1255 apportionment of fine aerosol at an urban site of Beijing using a chemical mass balance model, *Atmos.*
 1256 *Chem. Phys.*, 7321–7341, <https://doi.org/10.5194/acp-21-7321-2021>, 2021 ~~in preparation, Atmos.~~
~~*Chem. Phys. Discuss.*, <https://doi.org/10.5194/acp-2020-1020>, in review, 2020.~~

1257

1258 Xu, W., Sun, Y., Wang, Q., Zhao, J., Wang, J., Ge, X., Xie, C., Zhou, W., Du, W., Li, J., Fu, P.,
 1259 Wang, Z., Worsnop, D. R., and Coe, H.: Changes in aerosol chemistry from 2014 to 2016 in winter
 1260 in Beijing: Insights from high-resolution aerosol mass spectrometry, *J. Geophys. Res.-Atmos.*, 124,
 1261 1132-1147, 10.1029/2018JD029245, 2019.

1262

1263 Yan, C., Zheng, M., Sullivan, A. P., Shen, G., Chen, Y., Wang, S., Zhao, B., Cai, S., Desyaterik, Y.,
 1264 Li, X., Zhou, T., Gustafsson, Ö., and Collett, J. L.: Residential coal combustion as a source of
 1265 levoglucosan in China, *Environ. Sci. Technol.*, 52, 1665-1674, 10.1021/acs.est.7b05858, 2018.

1266

1267 Yu, L., Wang, G., Zhang, R., Zhang, L., Song, Y., Wu, B., Li, X., An, K., and Chu, J.:
 1268 Characterization and source apportionment of PM_{2.5} in an urban environment in Beijing, *Aerosol Air*
 1269 *Qual. Res.*, 13, 574-583, 10.4209/aaqr.2012.07.0192, 2013.

1270

1271 Zhang, Y., Ren, H., Sun, Y., Cao, F., Chang, Y., Liu, S., Lee, X., Agrios, K., Kawamura, K., Liu, D.,
 1272 Ren, L., Du, W., Wang, Z., Prévôt, A. S. H., Szidat, S., and Fu, P.: High contribution of nonfossil
 1273 sources to submicrometer organic aerosols in Beijing, China, *Environ. Sci. Technol.*, 51, 7842-7852,
 1274 10.1021/acs.est.7b01517, 2017.

1275

1276 Zhang, J. K., Cheng, M. T., Ji, D. S., Liu, Z. R., Hu, B., Sun, Y., and Wang, Y. S.: Characterization
 1277 of submicron particles during biomass burning and coal combustion periods in Beijing, China, *Sci.*
 1278 *Tot. Environ.*, 562, 812-821, <https://doi.org/10.1016/j.scitotenv.2016.04.015>, 2016.

1279

- Zhang, J.-J., Cui, M.-M., Fan, D., Zhang, D.-S., Lian, H.-X., Yin, Z.-Y., and Li, J.: Relationship between haze and acute cardiovascular, cerebrovascular, and respiratory diseases in Beijing, *Environ. Sci. Pollut. Res.*, 22, 3920-3925, 10.1007/s11356-014-3644-7, 2015^a.
- Zhang, J., Wang, Y., Huang, X., Liu, Z., Ji, D., and Sun, Y.: Characterization of organic aerosols in Beijing using an aerodyne high-resolution aerosol mass spectrometer, *Adv. Atmos. Sci.*, 32, 877-888, 10.1007/s00376-014-4153-9, 2015^b.
- Zhang, J. K., Sun, Y., Liu, Z. R., Ji, D. S., Hu, B., Liu, Q., and Wang, Y. S.: Characterization of submicron aerosols during a month of serious pollution in Beijing, 2013, *Atmos. Chem. Phys.*, 14, 2887-2903, 10.5194/acp-14-2887-2014, 2014.
- ~~Zhang, Y., Sun, J., Zhang, X., Shen, X., Wang, T., and Qin, M.: Seasonal characterization of components and size distributions for submicron aerosols in Beijing, *Sci. China Earth Sci.*, 56, 890-900, 10.1007/s11430-012-4515-z, 2013.~~
- ~~Zhang, R., Jing, J., Tao, J., Hsu, S.-C., Wang, G., Cao, J., Lee, C. S. L., Zhu, L., Chen, Z., Zhao, Y., and Shen, Z.: Chemical characterization and source apportionment of PM_{2.5} in Beijing: seasonal perspective, *Atmos. Chem. Phys.*, 13, 7053-7074, <https://doi.org/10.5194/acp-13-7053-2013>, 2013.~~
- ~~Zhang, Q., Jimenez, J. L., Canagaratna, M. R., Ulbrich, I. M., Ng, N. L., Worsnop, D. R., and Sun, Y.: Understanding atmospheric organic aerosols via factor analysis of aerosol mass spectrometry: a review, *Anal. Bioanal. Chem.*, 401, 3045-3067, 2011.~~
- Zhang, X., Hecobian, A., Zheng, M., Frank, N. H., and Weber, R. J.: Biomass burning impact on PM_{2.5} over the southeastern US during 2007: integrating chemically speciated FRM filter measurements, MODIS fire counts and PMF analysis, *Atmos. Chem. Phys.*, 10, 6839-6853, 10.5194/acp-10-6839-2010, 2010.
- Zhang, Y., Sheesley, R. J., Schauer, J. J., Lewandowski, M., Jaoui, M., Offenberg, J. H., Kleindienst, T. E., and Edney, E. O.: Source apportionment of primary and secondary organic aerosols using positive matrix factorization (PMF) of molecular markers, *Atmos. Environ.*, 43, 5567-5574, 2009.
- Zhang, Y., Schauer, J. J., Zhang, Y., Zeng, L., Wei, Y., Liu, Y., and Shao, M.: Characteristics of particulate carbon emissions from real-world Chinese coal combustion, *Environ. Sci. Technol.*, 42, 5068-5073, 10.1021/es7022576, 2008.
- Zhang, Y.-x., Min, S., Zhang, Y.-h., Zeng, L.-m., He, L.-y., Bin, Z., Wei, Y.-j., and Zhu, X.-l.: Source profiles of particulate organic matters emitted from cereal straw burnings, *Journal of Environmental Sciences*, 19, 167-175, 2007.
- Zhao, Z.-Y., Cao, F., Fan, M.-Y., Zhang, W.-Q., Zhai, X.-Y., Wang, Q., and Zhang, Y.-L. J. A. E.: Coal and biomass burning as major emissions of NO_x in Northeast China: Implication from dual isotopes analysis of fine nitrate aerosols, *Atmos. Environ.*, 242, 117762, 2020.
- Zhao, X., Hu, Q., Wang, X., Ding, X., He, Q., Zhang, Z., Shen, R., Lü, S., Liu, T., Fu, X., and Chen, L.: Composition profiles of organic aerosols from Chinese residential cooking: case study in urban Guangzhou, south China, *J. Atmos. Chem.*, 72, 1-18, 10.1007/s10874-015-9298-0, 2015.
- Zheng, M., Salmon, L. G., Schauer, J. J., Zeng, L., Kiang, C. S., Zhang, Y., and Cass, G. R.: Seasonal trends in PM_{2.5} source contributions in Beijing, China, *Atmos. Environ.*, 39, 3967-3976, <https://doi.org/10.1016/j.atmosenv.2005.03.036>, 2005.

1331
1332 Zhou, Y., Zheng, N., Luo, L., Zhao, J., Qu, L., Guan, H., Xiao, H., Zhang, Z., Tian, J., and Xiao, H.:
1333 Biomass burning related ammonia emissions promoted a self-amplifying loop in the urban
1334 environment in Kunming (SW China), *Atmos. Environ.*, 118138,
1335 <https://doi.org/10.1016/j.atmosenv.2020.118138>, 2020.
1336

1337 **TABLE LEGENDS**

1338 **Table 1.** List of the studies conducted in the Beijing metropolitan area to evaluate PM sources.

1339

1340 **FIGURE LEGENDS**

1341 **Figure 1.** Factor profiles for identified factors at IAP and PG. The bars show the composition
1342 profile (left axis) and the dots, the Explained Variation (right axis).

1343 **Figure 2.** Temporal variation of identified factors at IAP and PG. Solid and broken lines represent
1344 IAP and PG, respectively.

1345 **Figure 3.** Contribution of different sources to PM_{2.5} mass at IAP and PG.

1346 **Figure 4.** Correlations observed between PMF and CMB results at IAP. *If two outlying points
1347 are removed from the coal combustion-PMF, correlations are markedly improved.

1348 **Figure 5.** Correlations observed between PMF and CMB results at PG.

1349 **Figure 6.** Correlations observed between PMF and online AMS PMF results at IAP (winter). -*If
1350 two outlying points are removed from the coal combustion-PMF, correlations are
1351 markedly improved.

1352 **Figure 7.** Correlations observed between PMF and offline AMS PMF results at IAP (winter).

1353

1354

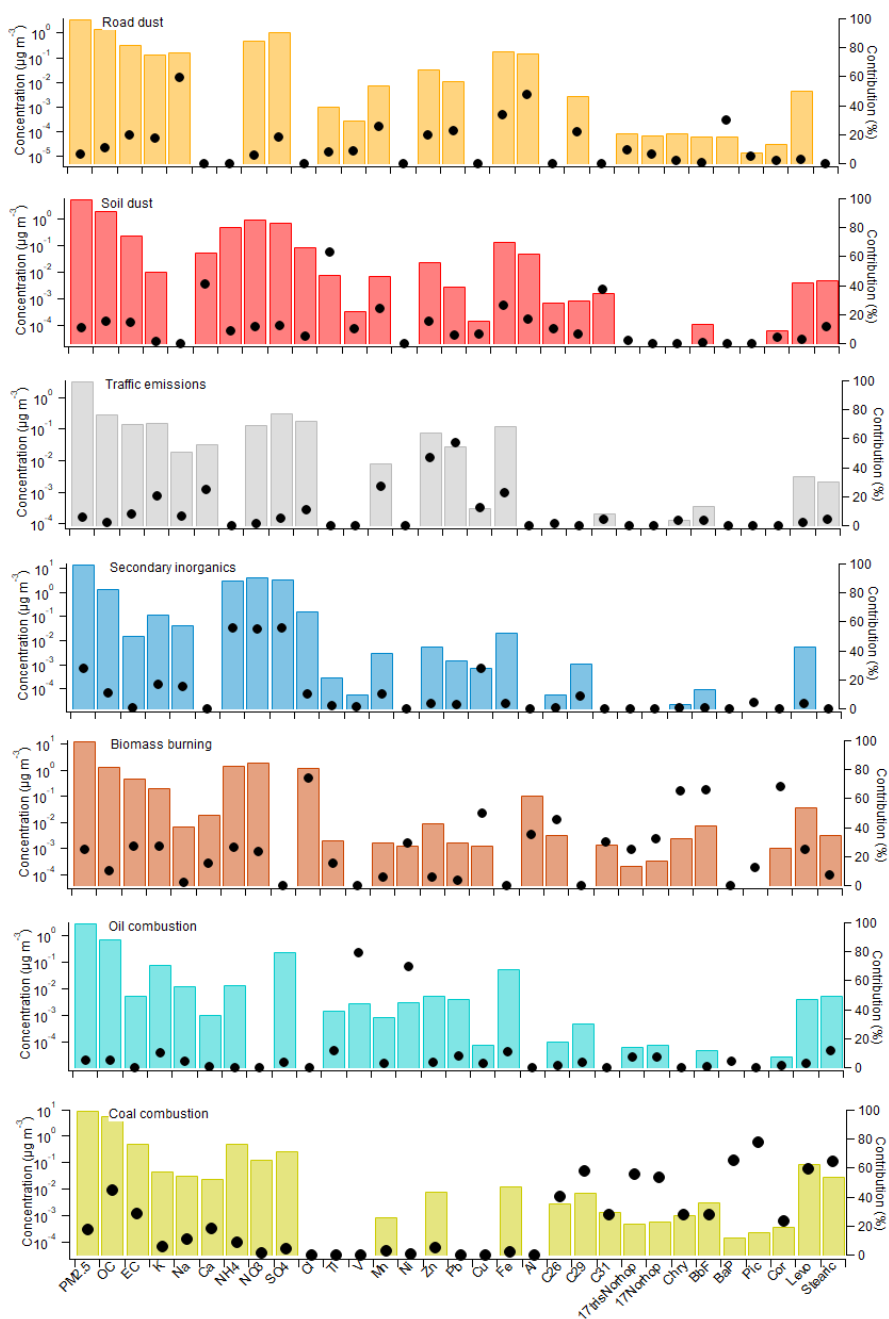
1355
1356

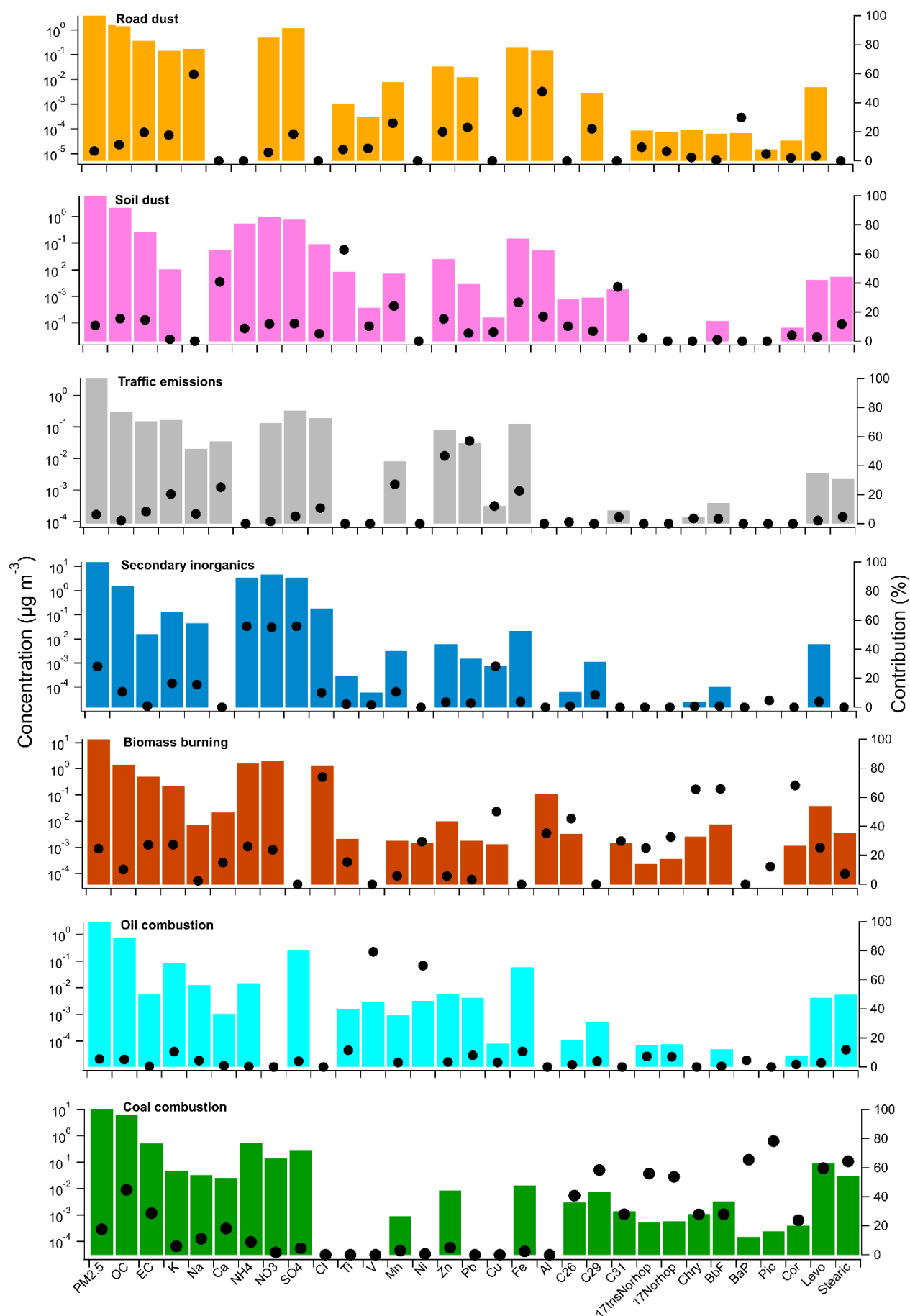
Table 1. List of the studies conducted in the Beijing metropolitan area to evaluate PM sources.

Reported Studies	PM-size fraction	Sampling site	Study period	Identified PMF factors (% contribution)						Input species
				Dust/soil dust ^a /road dust ^a /mineral dust ^a /local ^b /non-local ^c	Traffic/fossil fuel ^e	Coal combustion	Biomass burning	Secondary inorganics	Industrial	
Li et al. (2019)	PM _{2.5}	Urban-IAP	15 th Sep–12 th Nov 2014	-	-	-	-	-	-	Mg, Al, K, Ca and Fe; V, Cr, Mn; Co, Cu, Zn; Ag, Cd, Pb and As
		Suburban-UCAS	15 th Sep–12 th Nov 2014	-	-	-	-	-	-	
Liu et al. (2019)	PM _{2.5}	PKU	Nov–Dec 2016	5	18	16	9	44	8	OC, EC, NO ₃ ⁻ , SO ₄ ²⁻ , NH ₄ ⁺ , Cl ⁻ , Na ⁺ , Mg, Al, K, Ca, Ba, Cr, Mn, Fe, Ni, Cu, Zn, As, Se, and Pb
Ma et al. (2017a)	PM _{2.5}	Urban-IAP	24 th Feb–12 th Mar 2014	10 [±]	6	18 [±]	18 [±]	46	20	Na ⁺ , K ⁺ , Mg ²⁺ , Ca ²⁺ , NO ₃ ⁻ , SO ₄ ²⁻ , NH ₄ ⁺ , Cl ⁻ , Al, Fe, Ti, Mn, Cu, Zn, Sb, Pb, Cr, PM _{2.5} , EC, OC
Tian et al. (2016)	PM _{2.4}	Urban-IAP	Mar 2013–28 th Feb 2014	8.4 [±]	19.6	17.7	11.1	25.1	12.1	Na, Mg, Al, K, Ca, Mn, Fe, Co, Ni, Cu, Zn, Mo, Cd, Ba, Ti, Pb, Th, U, Na ⁺ , NH ₄ ⁺ , K ⁺ , Mg ²⁺ , Ca ²⁺ , Cl ⁻ , SO ₄ ²⁻ , NO ₃ ⁻ , OC and EC;
	PM _{2.4-9}		Mar 2013–28 th Feb 2014	10.9 [±] , 22.6 [±]	-	7.8	11.8	9.8	5.1	
Yu et al. (2013)	PM _{2.5}	Urban-BNU	1 st –Jan–31 st Dec 2010	12.7 [±] , 10.4 [±]	17.1, 16 [±]		11.2	26.5 [±]	6	Mg, Al, Si, P, S, Cl, K, Ca, Ti, V, Cr, Mn, Fe, Ni, Cu, Zn, As, Se, Br, Ba and Pb
Zhang et al. (2013)	PM _{2.5}	PKU	April, July, Oct 2009 and Jan 2010	16 [±]	3 [±]	14	13	26	28	Na ⁺ , K ⁺ , Mg ²⁺ , Ca ²⁺ , NO ₃ ⁻ , SO ₄ ²⁻ , NH ₄ ⁺ , Cl ⁻ , Al, Fe, Na, Mg, K, Ca, Ba, Co, Mo, Cd, Sn, As, Se, Rb, Ti, Mn, Cu, Zn, Sb, Pb, Cr, PM _{2.5} , EC, OC
Wang et al. (2008)	PM _{2.5}	Urban-BNU	Summer and winter	8.8 [±] , 6.7 [±]	5.9	16.7	11.8	12.7 [±] , 14.7 [±]	8.8	Na, K ⁺ , Mg ²⁺ , NO ₃ ⁻ , SO ₄ ²⁻ , NH ₄ ⁺ , Cl ⁻

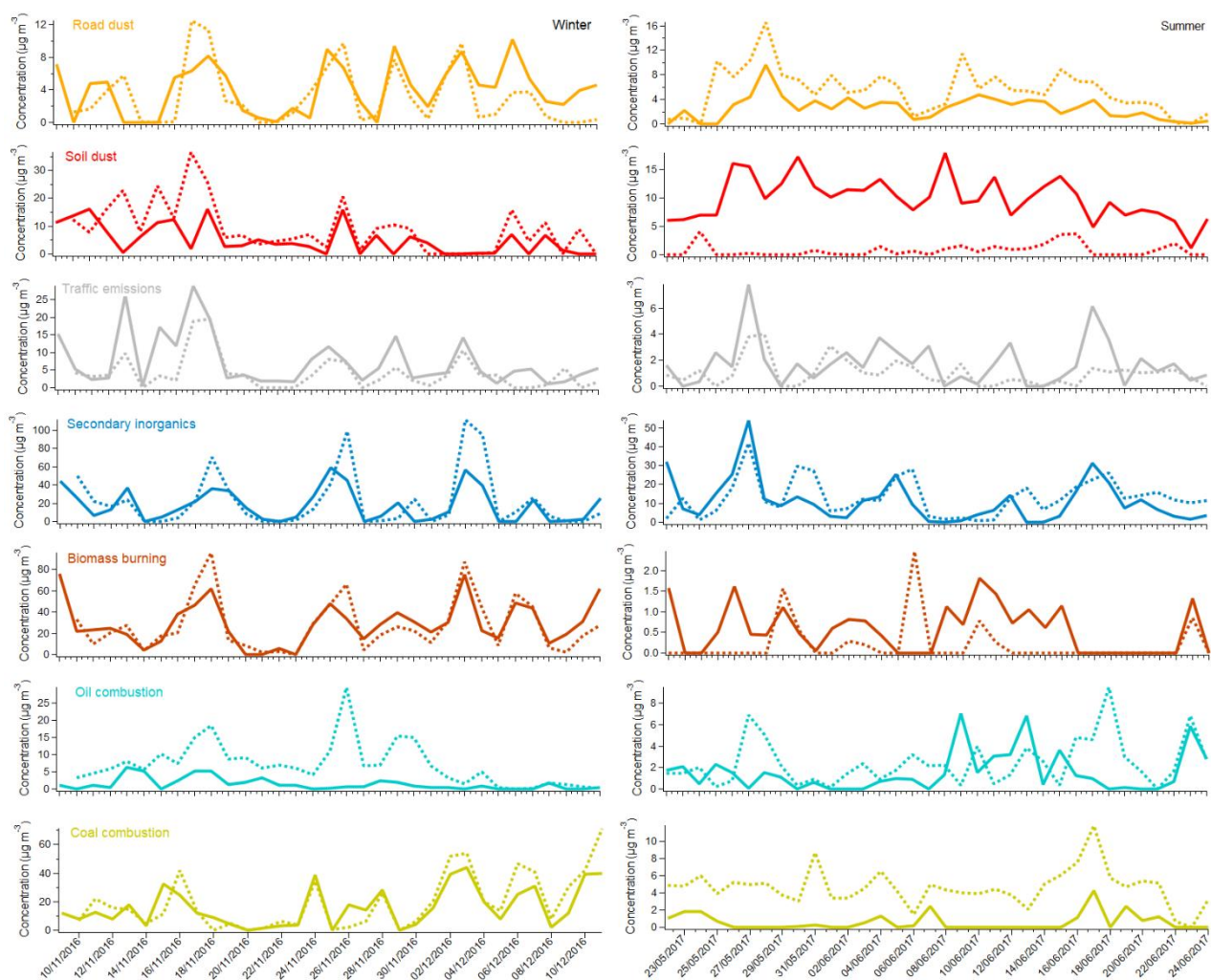
			2001 to 2006							Al, Fe, Na, Mg, K, Ca, Co, Cd, As, Ti, Mn, Cu, Zn, Sb, Pb, S, Cr, BC, OC, C ₂ O ₄ ²⁻
	PM ₁₀		Summer and winter 2001 to 2006	23 ^β	8.4	13.3	10.2	18.9	14.9	
	PM _{2.5}	Duolun [©]	Summer and winter 2001 to 2006	36.2 ^β ; 23.1 ^α	-	-	15.6	7.1 [*]	-	
	PM ₁₀		Summer and winter 2001 to 2006	61.7 ^β ; 11 ^α	-	-	18.1	4.1	-	
Song et al. (2007)	PM _{2.5}	Urban-PKU, OLC, SJS, TZ, and LX; Rural-MT	Jan 2004	7.8 [*]	8.5	40.6	16.4	9.2 [‡] ; 10.5 [*]	-	OC, EC, NO ₃ ⁻ , SO ₄ ²⁻ , NH ₄ ⁺ , Cl ⁻ , Na, Mg, Al, K, Ca, Ti, V, Cr, Mn, Fe, Ni, Cu, Zn, As, Se, and Pb
			Aug 2004	4.4 [*]	7.8	5.9	6.7	12.6 [‡] ; 4.2 [*]	-	
Song et al. (2006)	PM _{2.5}	OT, NB, BJ, XY, CH	6-day intervals in Jan, Apr, Jul, and Oct 2000	9 [*] and yellow dust	6	19	11	17 [*] ; 14 [*]	6	OC, EC, NO ₃ ⁻ , SO ₄ ²⁻ , NH ₄ ⁺ , Na, Al, Si, Cl, K, Ca, Ti, V, Cr, Mn, Fe, Ni, Cu, Zn, As, Se, Br, Pb, and Mg

⁺ Reported as traffic and waste incineration emissions; [‡] Secondary sulphur/^{*} secondary nitrate; ^β Fossil fuel; ^α Reported as combined coal and biomass burning contribution; [©] Background site; University of Chinese Academy of Sciences UCAS; Peking University PKU; Beijing Normal University BNU; Ming Tombs OT, the airport NB, Beijing University BJ, Dong Si EPB XY, and Yong Le Dian CH





1365 **Figure 1.** Factor profiles for identified factors at IAP and PG. The bars show the composition profile
 1366 (left axis) and the dots, the Explained Variation (right axis).
 1367
 1368



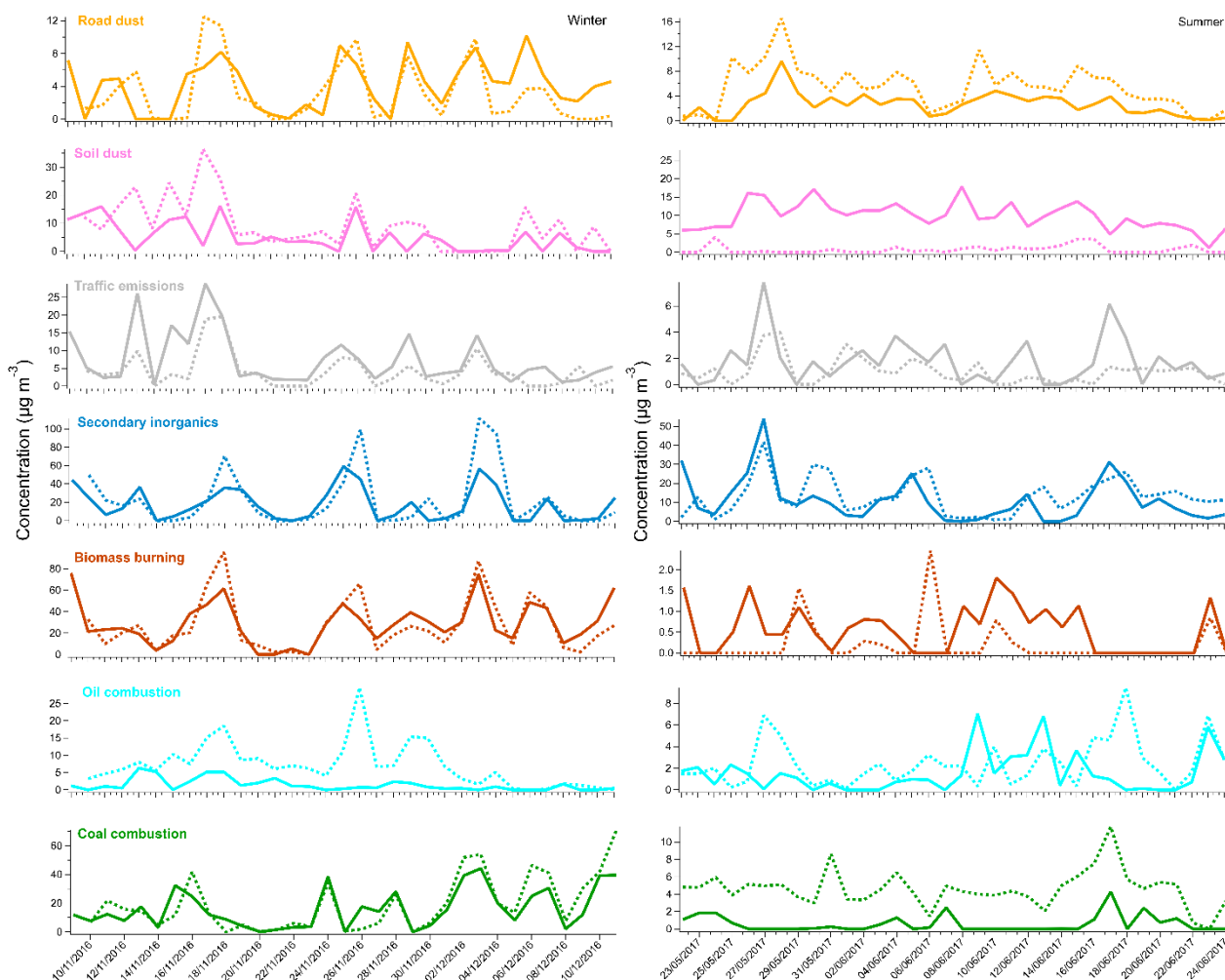
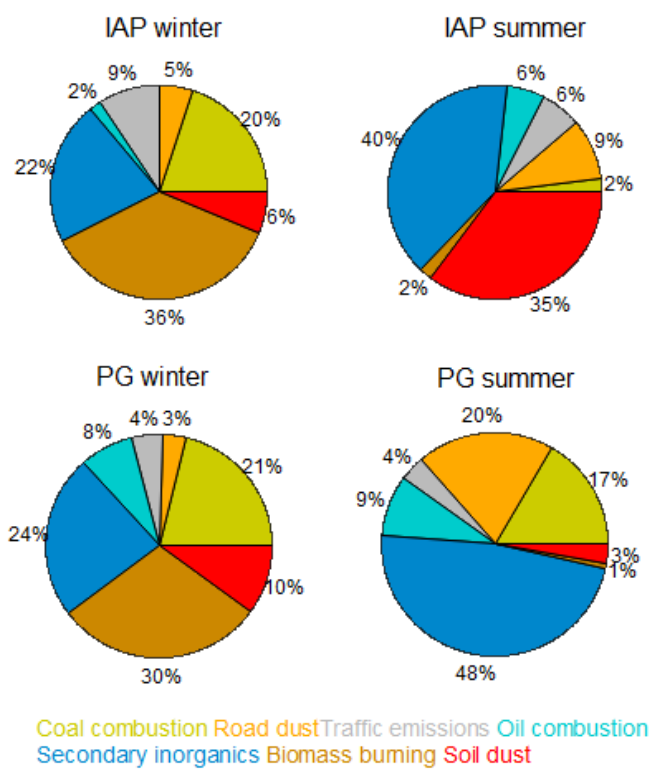


Figure 2. Temporal variation of identified factors at IAP and PG. Solid and broken lines represent IAP and PG, respectively.



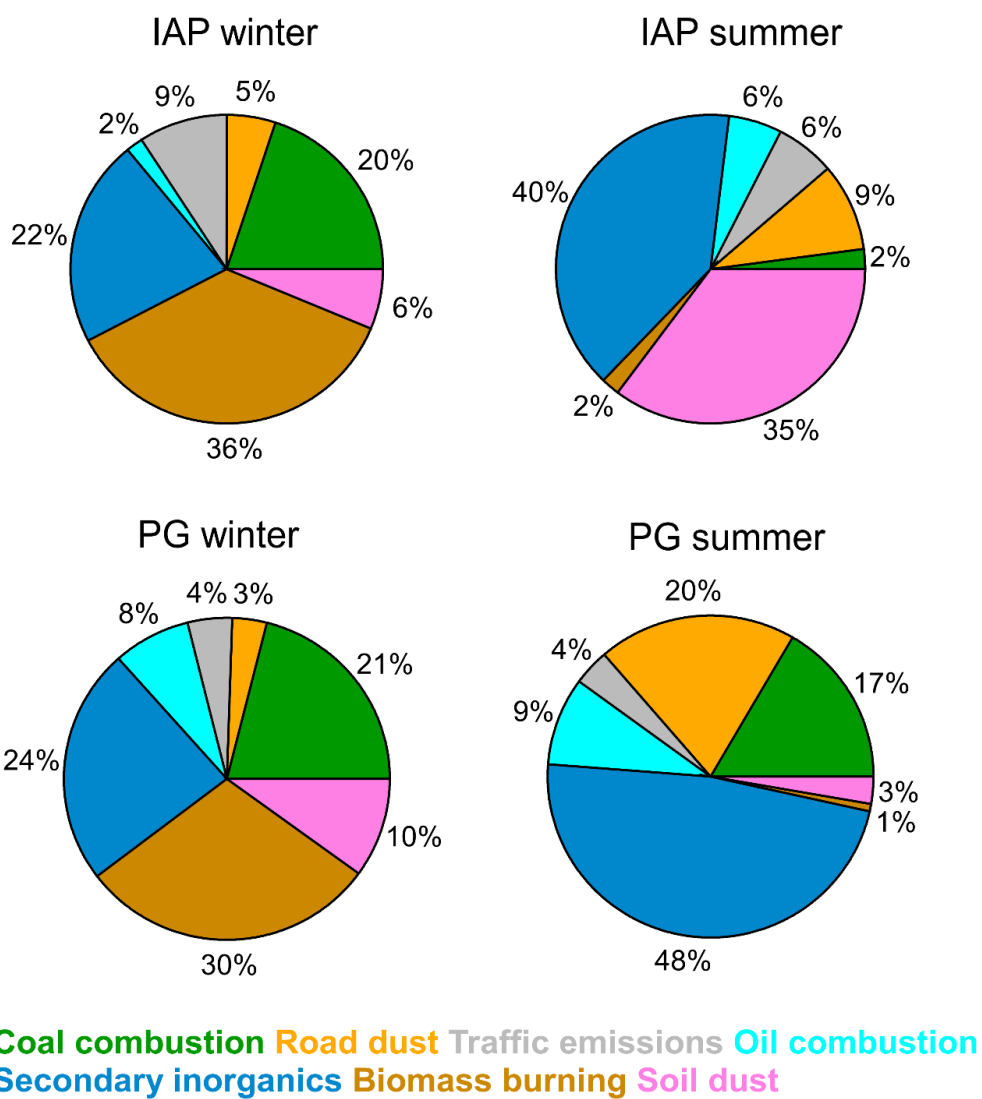
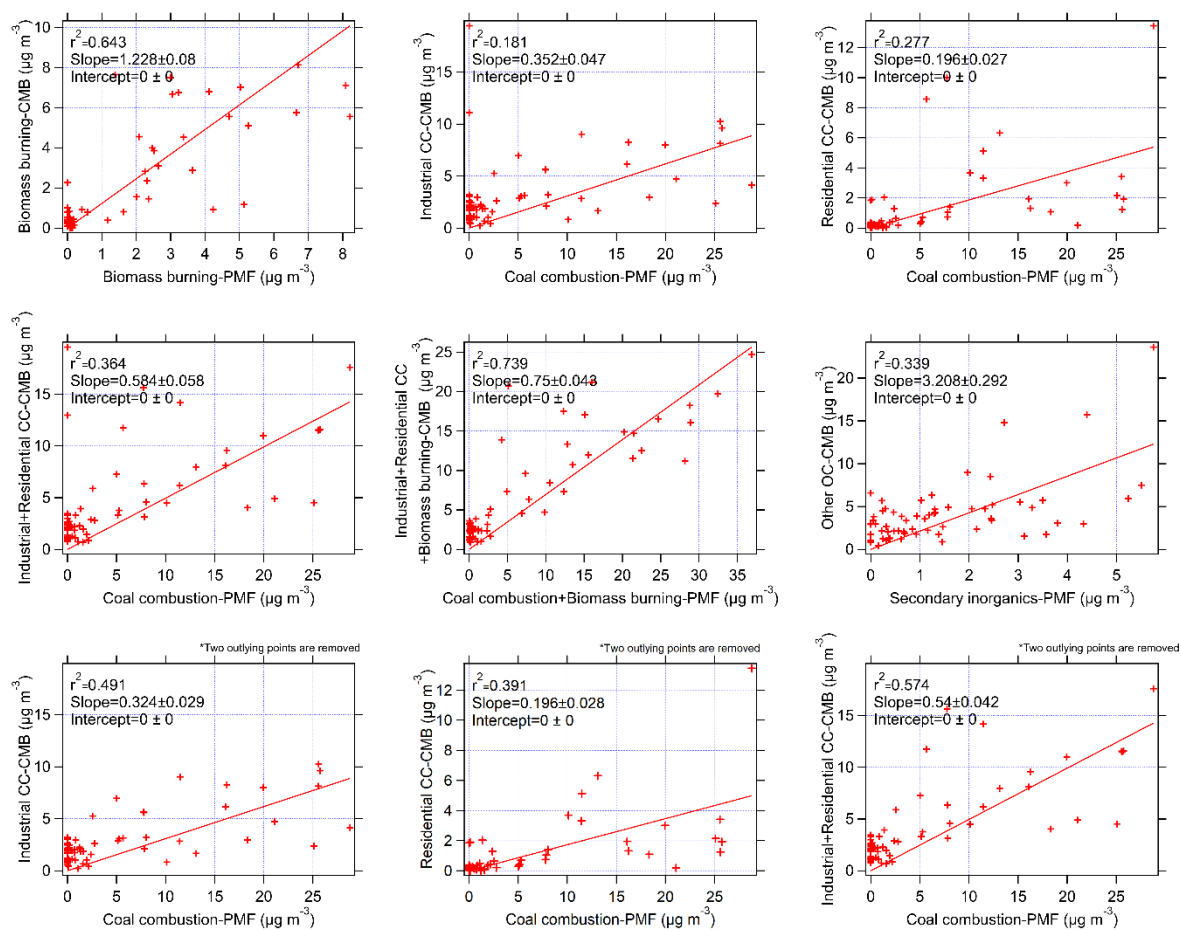


Figure 3. Contribution of different sources to PM_{2.5} mass at IAP and PG.

1378

1379



1380

1381 **Figure 4.** Correlations observed between PMF and CMB results at IAP. *If two outlying points are removed
1382 removed from the coal combustion-PMF, correlations are markedly improved.

1383

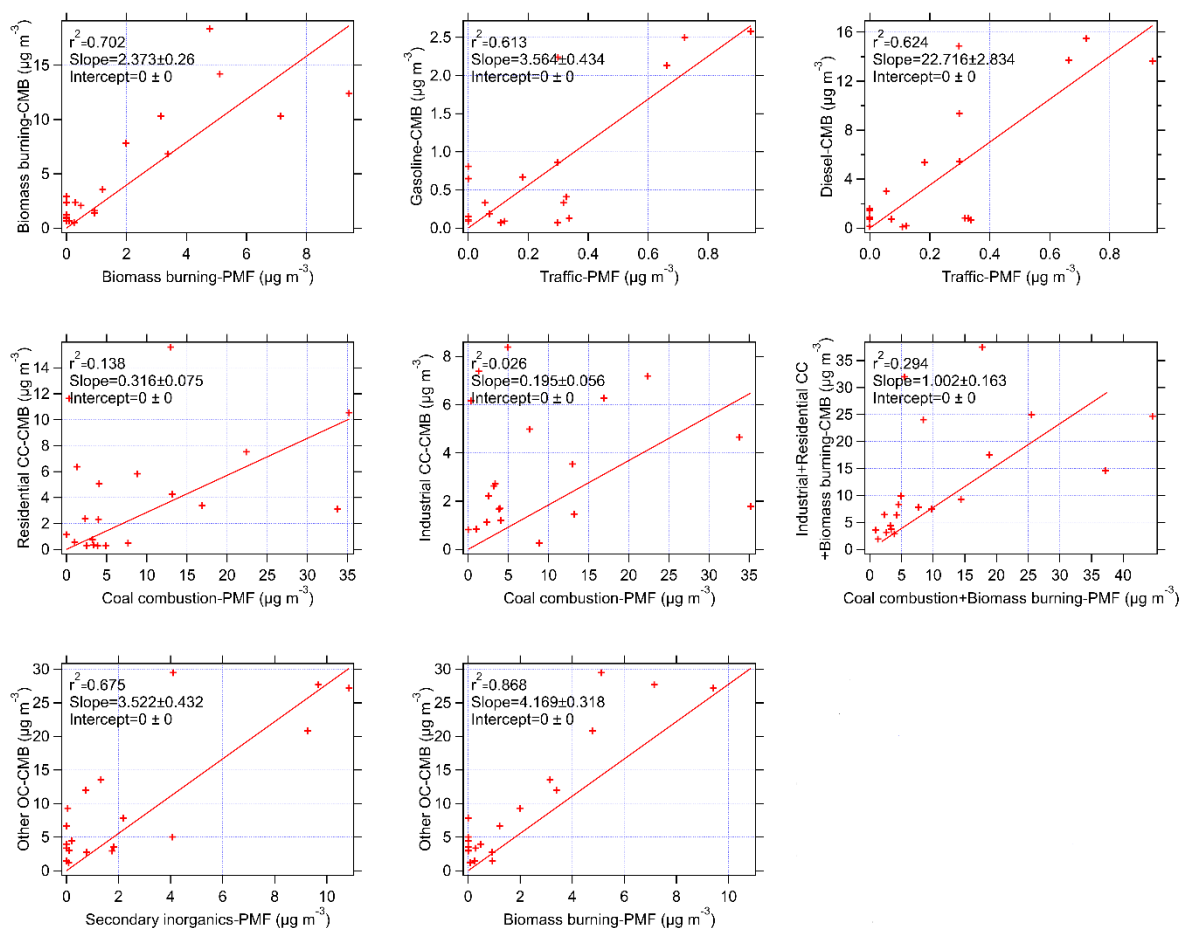


Figure 5. Correlations observed between PMF and CMB results at PG.

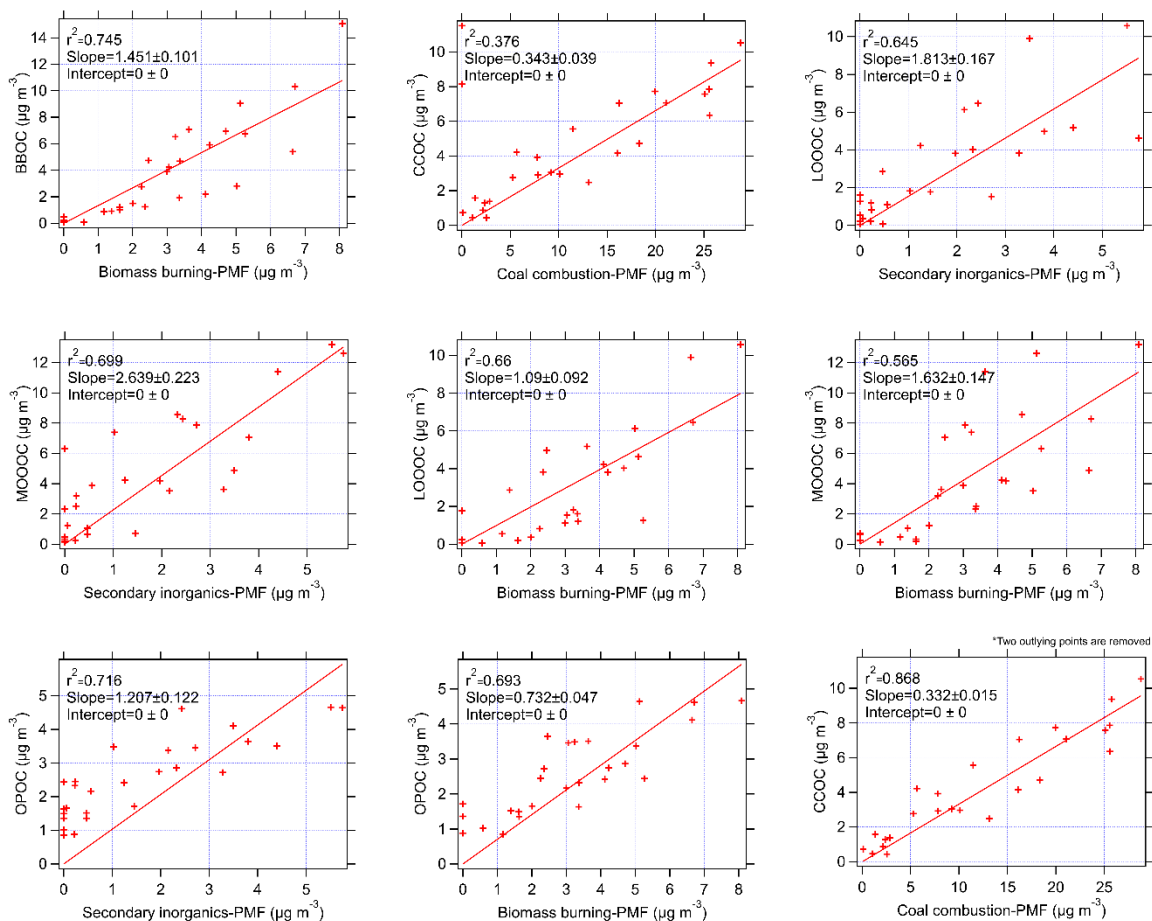
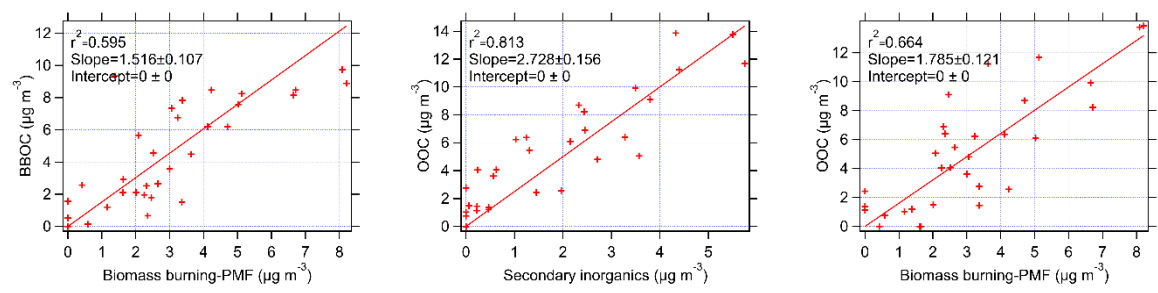


Figure 6. Correlations observed between PMF and online AMS PMF results at IAP (winter).- *If two outlying points are removed from the coal combustion-PMF, correlations are markedly improved.

1391



1392

1393 **Figure 7.** Correlations observed between PMF and offline AMS PMF results at IAP (winter).

1394

1395